



Mercator Ocean

Ocean Forecasters

SPECIAL ISSUE
with
Coriolis



The Tara Oceans voyage took place on the schooner "Tara" from 2009 to 2013 and visited all oceans to collect samples and data in order to study the relationships between ecosystem biodiversity and function and the physical-chemical oceanographic environment (water mass, transport) (cf Picheral et al. this issue).

Credits: Francois Aurat/Tara Expéditions; Marc Picheral/LOV/CNRS/Tara Oceans; Stéphanie Januskiewicz/Tara Expéditions

Editorial - May 2014 - Special Issue jointly coordinated by Mercator Ocean and Coriolis focusing on Ocean Observations

Greetings all,

Once a year and for the fifth year in a row, the Mercator Ocean Forecasting Center in Toulouse and the Coriolis Infrastructure in Brest publish a common newsletter. Some papers are dedicated to observations only, when others display collaborations between the 2 aspects: Observations and Modelling/Data assimilation.

The first paper by Cabanes et al. introducing this issue is presenting a new methodology aiming at correcting Argo float salinity measurements in delayed time when Argo floats conductivity sensors are subject to drift and offset due to bio-fouling or other technical problems.

Then, Cravatte et al. are using the Argo arrays in order to compile Argo floats' drifts and show that they are a very valuable tool allowing determining the absolute velocity. They apply this to study zonal jets at 1000 meters depth in the Tropics.

In the next paper, Maes and O'Kane provide with some results indicating the impact of a sustained ocean observing Argo network on the ability to resolve the seasonal cycle of salinity stratification by contrasting periods pre- and post-Argo. They take into account the respective thermal and saline dependencies in the Brunt-Väisälä frequency (N^2) in order to isolate the specific role of the salinity stratification in the layers above the main pycnocline.

Picheral et al. are telling us about the Tara Oceans voyage that took place on the schooner "Tara" from 2009 to 2013 and visited all oceans. The ship was adapted for modern oceanography. Scientific instruments were mounted on a dedicated CTD frame and installed on an underway flow-through system. Data were sent daily to Coriolis. Post cruise calibrations were performed leading to a high quality dataset.

Then, Roquet et al. demonstrate the importance of the contribution of hydrographic and biogeochemical data collected by Antarctic marine mammals, and in particular elephant seals, equipped with a new generation of oceanographic tags, for the environmental monitoring of the Southern Ocean.

The last paper of the present issue is displaying the collaboration between the Ocean Observations and Ocean Modelling communities: Turpin et al. perform several Observing System Experiments in order to assess the impact of Argo observations on the Mercator Océan global analysis and forecasting system at $\frac{1}{4}$ degree resolution.

We wish you a pleasant reading,

Laurence Crosnier and Sylvie Pouliquen, Editors.

Table of Content:

1. DELAYED MODE ANALYSIS OF ARGO FLOATS: IMPROVEMENTS OF THE METHOD IN THE NORTH ATLANTIC AND SOUTHERN OCEAN	3
<i>By C. Cabanes, V. Thierry, J. Lepasqueur, S. Speich, C. Lagadec</i>	
2. ZONAL JETS AT 1000M IN THE TROPICS OBSERVED FROM ARGO FLOATS' DRIFTS	11
<i>By S. Cravatte, F. Marin, W. S. Kessler</i>	
3. UPPER OCEAN SALINITY STRATIFICATION IN THE TROPICS AS DERIVED FROM N2, THE BUOYANCY FREQUENCY	15
<i>By C. Maes, and T. J. O'Kane</i>	
4. MONITORING THE OCEAN WITH TARA - A CORIOLIS PERSPECTIVE	20
<i>By M. Picheral, H. Legoff, V. Taillandier, S. Searson, C. Marec, G. Obolensky and S. Morisset</i>	
5. ELEPHANT SEALS HELP US TO BETTER OBSERVE THE SOUTHERN OCEAN	26
<i>By F. Roquet, S. Blain, C. Guinet, G. Reverdin</i>	
6. OBSERVING SYSTEM EXPERIMENT: A SIMPLE TOOL TO ASSESS THE MULTIPLE ROLES PLAYED BY ARGO OBSERVATIONS ON THE OPERATIONAL FORECASTING SYSTEM OF MERCATOR OCÉAN	29
<i>By V. Turpin, E. Remy, P-Y Le Traon</i>	

Delayed Mode Analysis of Argo Floats: improvements of the method in the North Atlantic and Southern Ocean

By C. Cabanes⁽¹⁾, V. Thierry⁽²⁾, J. Lepasqueur⁽¹⁾, S. Speich^(3,4), C. Lagadec⁽²⁾

¹ CNRS/UMS3113, Brest, France

² IFREMER/LPO, Brest, France

³ UBO/ LPO, Brest, France

⁴ ENS/LMD, Paris, France

Abstract

Argo floats conductivity sensors can be subject to drift and offset due to bio-fouling or other technical problems. Several approaches have been proposed in order to correct the float salinity measurements in delayed time. The method developed by Owens and Wong 2009 (OW, 2009) is now widely used by the Argo community. However, our experience has shown that it is sometimes difficult to detect a float salinity drift or offset in the North Atlantic and the Southern Ocean around southern Africa only on the basis of the results from OW method and that it can be necessary to use complementary approaches. In this study we have shown that some modifications of the standard OW method are necessary in both regions in order to gain confidence in the results proposed by the method and to make it easier for the PI of the float to decide whether a salinity correction is necessary. In the North Atlantic, we have slightly modified the OW method in order to better take into account the large decadal/interannual variability of the large scale salinity field which is assumed to be constant in the standard method. Additional modifications have been implemented for the Southern area in order to better take into account the presence of fronts and large eddy variability. Particularly, in this area, we implemented a new methodology that takes into account the comparison with historical data water-masses properties such as variable theta-related depths and the dynamic height of the Argo profile. In the North Atlantic, the modified OW method has been used to check the consistency of the corrections previously applied on the float salinity data.

Introduction

Argo floats drift freely at preset parking depths and measure temperature, salinity, and pressure with a conductivity-temperature-depth (CTD) sensor during their ascent to the sea surface every ten days. At the sea surface, they relay the observed data to shore via satellites before returning to their parking depth. The Argo target accuracies for measurement are 5 dB for pressure, 0.005°C for temperature, and 0.01 PSU for salinity (Argo Science Team, 2000). Whereas the two first objectives could be achieved, the third one for salinity is harder to achieve because conductivity cells get sometimes contaminated as a result of biological fouling, or experience other technical problems. Then, salinity measurements are sometimes subject to artificial trends or offset.

Maintaining the quality of salinity data is critical for the Argo Project. PIs or delayed mode operators from regional data centers are asked to perform delayed mode analysis of their floats. Basically, floats are analyzed in delayed time at least once year after deployment. Several methods have been developed in order to evaluate the performance and correct the errors of the ARGO salinity sensors in the ocean. Among them, the "direct method" (i.e. recovery of the float and post-calibration of the sensor) has proven to be valuable (Oka and Ando, 2004, Oka, 2005) but remains very rarely applied and costly. The more common method is then to compare Argo salinity profile with reference measurements (nearby CTDs or already calibrated Argo profiles). At the beginning of the Argo project, efforts have been devoted to standardize delayed mode procedures of salinity correction. These procedures have been written (and regularly updated) in the Argo quality control manual (Version 2.9 Wong et al, 2013). Up to now, three softwares are freely available to the Argo community for detecting and correcting salinity sensor drift or offset. The first one was originally developed by Wong et al. (2003). This method was significantly improved by Böhme and Send (2005), particularly in highly variable environments and regions where the flow is bathymetrically controlled such as the Subpolar North Atlantic. Later on, Owens and Wong (2009) (OW) proposed a method that combined improvements to the optimal interpolation and the fitting procedure from both previous methods. OW method is now widely used by the Argo community and is thought to suit float data for the Global Ocean. Together with the method, two reference databases are distributed and regularly updated. The first database contains historical CTD data; the other one contains historical Argo profiles that do not have any salinity adjustment in delayed time.

However, our experience has shown that sometimes it can remain a challenge to detect a float salinity drift or offset in the North Atlantic and the Austral Ocean only on the basis of the results from OW method:

- Indeed, in the North Atlantic, complex water mass structures and basin bathymetry, rapid timescales of change require special care in mapping salinity using historical data. Moreover, significant interannual and decadal variability is observed in many processes that influence the circulation and water properties. Particularly, recent warming and salinification of the main intermediate and deep waters formed in the northern North Atlantic have been reported (Sarafanov et al., 2007). For example, Labrador Sea Water (LSW) in the Irminger sea became saltier by 0.04 PSU on average for the period between 1997 and 2006, while in the Iceland Basin, the LSW became saltier by 0.01 PSU after 2002 (Sarafanov et al., 2007). These recent changes in salinity may make it difficult to compare floats data (acquired in the 2000's) to historical reference CTD data as even the deepest float measurements could have been subject to significant interannual to decadal changes. For example, part of the floats deployed between Portugal and Greenland during the OVIDE cruises flow in the Subpolar North Atlantic and has been processed in delayed mode by our team. The comparison of the salinity of these floats with reference CTD data using the OW method often suggests that the float salinities are biased toward too salty values. However, this was not confirmed by the comparison of the float data with the CTD made at launch or by close inspection of the float salinity profiles. Therefore, for many of the OVIDE floats, we have considered that the float salinity measurements were not biased and we have decided not to apply the correction suggested by the OW method.

- The Southern Ocean is the most energetic region in the world's oceans. As a result, it is a location of high lateral variability of water masses that are separated by relatively small-scale very variable dynamical features as frontal jets, eddies, meanders and filaments. This is particularly true south of Africa, where is observed the largest turbulence in the ocean. In this region the eastward flowing Antarctic Circumpolar Current and South Atlantic Current meet with the westward injection of flowing Indian waters carried by the Agulhas Current and the Agulhas Retroflexion. At the same time, the Southern Ocean is poorly sampled, not least because of its harsh climate and remote location. Yet the spatial and temporal variation of water masses in this region plays an important part in the large-scale ocean circulation and climate. This is the reason that brought us to initiate in 2004 the GoodHope Clivar International program of repeated hydrographic cruises and Argo profiles deployment. In particular France has deployed more than 150 profiling floats. NOAA-AOIML, UK and Germany joined our effort. However, because of the highly turbulent dynamics of the region, the scarcity of hydrographic data, and the particular nature of local water masses properties, we found it impossible to implement the OW method as is.

The objective of this study is to verify whether the OW method could be tuned in the North Atlantic and the Southern Ocean in order to obtain results in accordance with the final PI decisions, namely a correction close to zero (within an error bar) if a PI decided not to correct a float for a salinity bias or drift. For this purpose, in both regions, we have selected floats that have been processed in delayed mode and for which no correction for a salinity drift or bias was judged necessary. Improvements of the standard OW method have been found to be necessary in the two regions and are detailed below.

The standard OW method

The OW method is a tool that can be divided into three main steps:

1. The selection of reference salinity profiles close to the Argo profiles (the selection criteria are relative to the pre-defined large length scales, short length scales and temporal scales). The topographic potential vorticity is included as an optional constraint in the calculation of the distance between points (cross-isobaths scale). Separation criteria can be used when a float crosses the Sub-antarctic Front (SAF). These criteria, based on the study of Sallée et al, 2008 select historical data from the same side of the SAF as the Argo profile, preventing mixing historical data from north and south of SAF.

2. A vertical interpolation of the reference (historical) salinity data onto the float observed potential temperatures (float θ levels) and a two-step optimal interpolation (OI) process to obtain an 'objectively mapped' salinity at the float location. First, a large scale field is estimated on each float θ level, using the set of reference salinities. The Gaussian decay for the covariance matrix is determined by large spatial scales and large cross-isobaths scale, assuming that the large scale field is time-independent. Then, this large scale field is subtracted from the reference salinity data. Residual are used to estimate the small scale field. In this case, the Gaussian decay for the covariance matrix is determined by the temporal scale, the small spatial scales and the small cross-isobaths scale. The 'objectively mapped' salinity is the sum of the large scale estimate S' and the small scale estimate S'' . The OI process also provides an error on the objectively mapped salinity. This mapping error is taken from the second stage map. It will be larger if the signal variance of residual from the large scale mapping is large and if contemporaneous data are not available or far away from the float position compared to the small spatial scales.

3. The estimation of the time-varying conductivity correction. All the salinity values from the floats and the objectively mapped salinities are converted to potential conductivity. The float conductivity data are then fitted to the 'objectively mapped' conductivity using a piece-wise linear fit. The calibration model is weighted by the inverse of the mapping error variance. The number of points of comparison in the vertical is restricted to 10 θ levels below the variable surface layers. The 10 θ levels are the θ surfaces in the float time series that have the minimum salinity variance on θ . The method provides an error on the fit assuming vertical correlation between data points (θ levels) but lateral independency

Improvements the standard OW method in the North Atlantic region (North of 30°N)

Selection of the floats

For each profile of each float that has been processed in delayed mode in the North Atlantic region, we have calculated the vertical mean difference between the raw salinity profile and the adjusted salinity profile obtained in delayed mode (PSAL - PSAL ADJUSTED). In case no salinity correction was necessary, the adjusted profile is simply equal to the raw profile. Therefore, a float was selected when the mean (PSAL - PSAL ADJUSTED) was lower than 0.002 PSU for each profile. The small tolerance of 0.002 PSU was set to allow the selection of floats that had a rather small adjustment on the raw pressure and for which the adjusted salinity had been computed in accordance with the adjusted pressure but with no further salinity corrections. Finally, we have excluded from the list all the SOLO floats with FSI sensors. In the North Atlantic, we have then selected 392 floats which salinity does not need to be corrected in delayed mode according to the PI's decision. This subset of 'unbiased' floats has been used to test the standard OW method in this region.

Results of the standard OW method

The standard OW method, with special settings for the North Atlantic region (see Böhme and Send, 2005), was run for the subset of 392 floats using the historical CTD reference database or both the historical CTD and Argo reference databases. The differences between mapped salinities and float salinities averaged over ten θ levels of a profile are shown on Figure 1a and Figure 1b. One would expect that the differences obtained for our subset of 'unbiased' floats would be distributed around zero. However, this is not the case, particularly along the Reykjanes Ridge and the topography of the Labrador Sea where systematic negative differences are found and in the western part of the Subtropical Gyre where systematic positive differences are found. These systematic differences are obvious when the Argo measurements are compared to the historical CTD reference database (Figure 1a) but are still apparent when the Argo measurements are compared to the more recent reference database (Figure 1b). Given these differences, the

corrections proposed by the OW method (when an offset is fitted) are often negative in the Subpolar region and positive in the Subtropical region in both cases. Moreover, the error on the proposed offset is very low and well below the instrument accuracy (0.01 PSU). Indeed, for 60% of the floats, the errors on the fit are less than 0.001 PSU and for 90 % of the floats, less than 0.003 PSU. Then, this statistical error does not help to discriminate significant offsets or drifts.

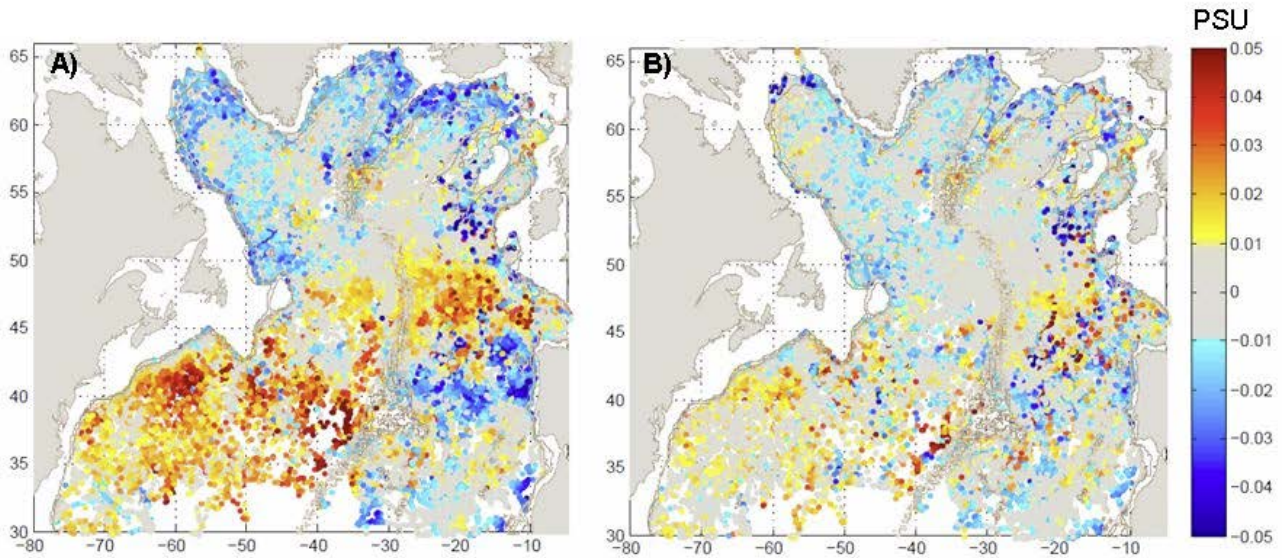


Figure 1: Differences (in PSU) between mapped salinities and float salinities averaged over 10 θ levels of a profile. A) CTD reference database is used B) ARGO+CTD reference databases are used.

Example of the float 5902269, in the Subpolar North Atlantic

The OVIDE float 5902269 is a PROVOR float launched in 2010. The float is still active and up to now, 108 cycles have been reviewed in delayed mode. From the PI's decision, this float does not present any salinity drift or bias. The comparison with the reference CTD database performed by the OW method tends, however, to propose a negative correction for salinity (see Figure 2). When the same float is compared to the more recent Argo reference database, the OW method also proposes a negative correction (although less negative than before), which suggests that there is a saline bias particularly along the topography of the Labrador Sea.

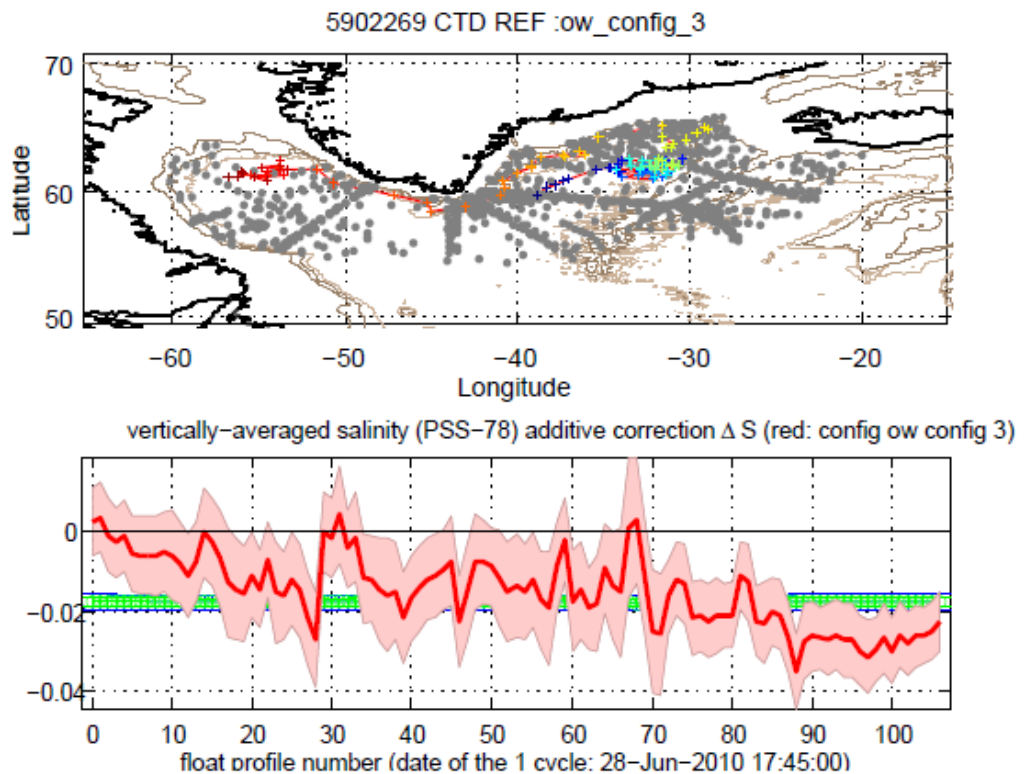


Figure 2: Results of the OW method. Reference CTD profiles used for the mapping (grey dots) are shown on the map (upper panel) along with the float trajectory. Vertically-averaged mapped salinities minus float salinities on 10 θ levels and the mapping errors (red). The offset obtained by the linear fit is shown (green circles) as well as 1x error on the fit (green error bars) and 2x error on the fit (blue error bars).

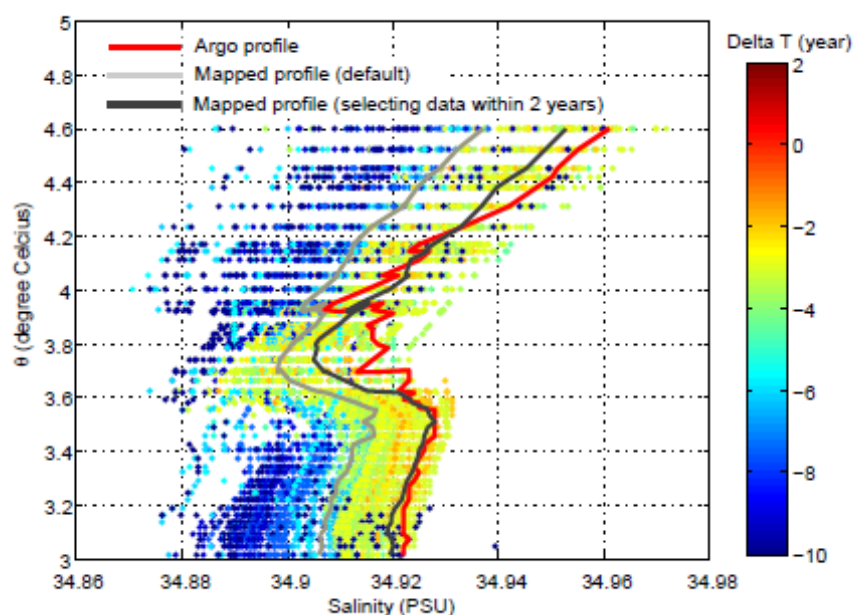


Figure 3: Profile 90 of the Argo float 5902269 (red) and the mapped profile obtained using the full Argo reference database (grey) and selecting data within 2 years of the float profile (black). Reference profiles used for the mapping are plotted with a color that represents Δt (year) = Date Argo profile - Date reference profile.

We have further investigated why negative differences are found between mapped salinities and the float salinities, particularly along the topography of the Labrador Sea. Figure 3 shows the reference profiles used for the mapping of the profile 90 of the float 5902269. This profile 90 was made in the Labrador Sea, near 50°W. They are plotted with a color that represents the difference between their date and the date of the Argo profile.

The interannual/decadal variability is quite high in this region. The mapped salinities differ from the Argo salinities by an amount of 0.01-0.02 PSU at all levels and look more like an average of all the historical salinities (without giving more weight to more recent data). To try to get a better estimate of the salinity, we have selected the reference profiles acquired within 2 years of the Argo profile. All the reference profiles outside the +/- 2 years interval were excluded from the analysis. We have then processed the OW method as before, keeping the parameters unchanged. The mapped salinity profile is plotted on Figure 3 and is now much closer from the Argo profile because the oldest reference profiles were not used.

We have then investigated why the mapping method does not give more weight to the most recent data. The mapping method processes in two stages. The first one maps the large scale field (with map scales of 2-3°) at the float profile location. This large scale field is assumed to be time independent and then, the large scale weights do not depend on the date of the historical profiles but only on the distance from the float position and the topographic potential vorticity. The time independent large scale field of salinity is also mapped at each reference profile location and residuals are used to map the small scale field (with map scales of 0.5-0.8°) in the second stage of the Optimal Interpolation. The small scale field is assumed to be time dependent with a time scale ($\tau = 0.69$ yr) that represents rather slow (seasonal to interannual) water mass changes. For the profile 90 of the float 5902269, small scale weights are very small and the contribution of the small spatial scales and recent reference profiles is very low on the final estimate compared to the contribution of the large scales. Indeed, the salinity estimate S at the level $\theta = 3.37^\circ\text{C}$ is $S = S' + S'' = 34.9124 - 0.0002$, with S' is the large scale estimate and S'' is the small scale estimate. The same is observed at all depths and, finally, the most recent reference profiles have very little influence and the mapped salinity mostly reflects an average salinity over 2003-2011 in this region.

Modifications of the standard OW method

The first solution that we have tried was to run the OW method, keeping the same configuration parameters as the standard ones, but selecting only the reference data within +/- 2 years of each Argo profile. Overall, the corrections proposed by the method are more distributed around zero than for standard configurations in the North Atlantic. However, we found cases where the mapping error is badly estimated because very few reference data are available within +/- 2 years of some Argo profiles. This can give rise to very low mapping errors for few profiles in a float time series. As a consequence, the calibration model (here the offset fit), weighted by the inverse of the mapping error variance, is pushed toward values with a very low mapping error and, therefore, is also badly estimated.

The chosen solution was to add a Gaussian decay with a time scale of 2 years in the large scale mapping stage in order to increase the weight of contemporaneous data when the large scale field is estimated. This time scale reflects that the large scale field is not time independent as assumed in the standard OW method. For the standard OW method, the mapping errors are taken from the small scale mapping stage only. In order to take this into account the computation of the mapping errors was modified, now including the errors from the large scale mapping stage.

The error on the fit (model error) is based on the error covariance of the data. As for the original OW method, the error covariance matrix is constructed assuming a vertical covariance between the various θ levels. In our modified version we have also assumed a lateral covariance between climatological profiles. This lateral covariance takes into account that a mapped profile on an Argo position is build from a set of reference profiles that is not very different from the subset used to build the mapped profile at the next or previous Argo profile position. This lateral covariance between two mapped profiles is constructed using a Gaussian function with a decay determined by the large spatial scales.

Results of the modified OW method

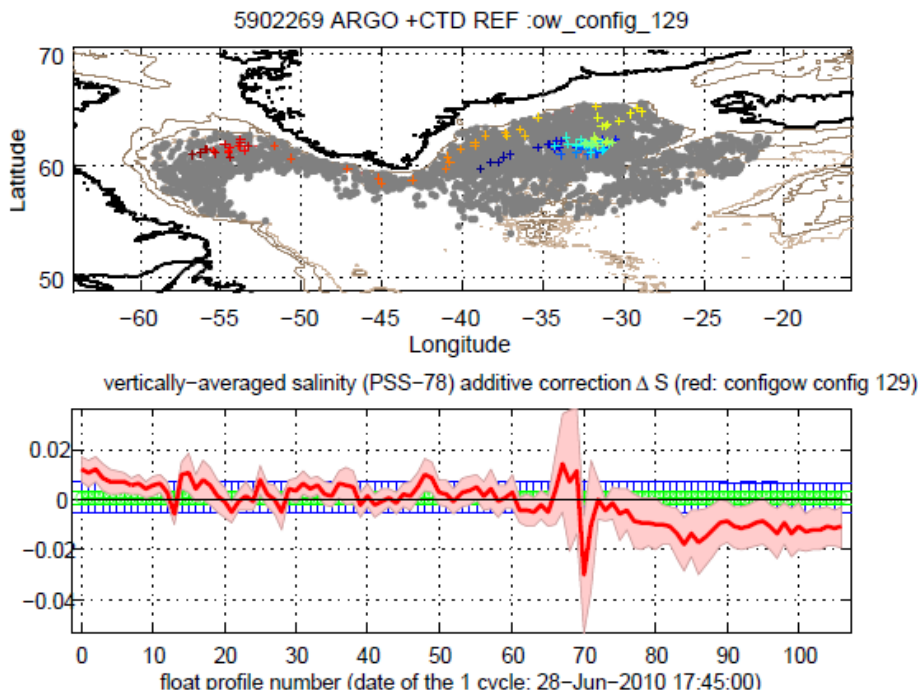


Figure 4: Results of the OW method for the configuration 129. Reference CTD and ARGO profiles used for the mapping (grey dots) are shown on the map (upper panel) along with the float trajectory. Vertically-averaged mapped salinities minus float salinities on 10 θ levels (red) and the computed offset (green)

We have run the OW method with the modifications presented above for the float 5902269 and all the other unbiased floats that we have been selected in the North Atlantic. The results for the float 5902269 are shown on the Figure 4. The mapping errors are larger at the end of the float time series, where we know that there are only few reference data within +/- 2 years of the date of the Argo profiles. Then, the mapped salinities at the end of the float time series have less influence on the final offset estimate. The errors on the final offset estimate are larger than for the standard OW method (Figure 2) and this is mainly due to the introduction of a lateral covariance between climatological profiles. The differences between mapped salinities and float salinities for the subset of 392 'unbiased' Argo floats do not show strong systematic biases (see Figure 5A) as it was the case before. The corrections proposed (see Figure 5B) are closer to zero which is much more consistent with the PI's decisions. The errors on the offsets are also larger than for the standard configuration.

Among the 392 floats, we have found 18 floats for which the correction proposed is larger than 0.01 PSU (or smaller than -0.01 PSU). For four of them (float numbers 6900162, 6900176, 6900515 and 6900614) we think that the delayed mode correction should not have been zero and should be revised (2 corrections have been revised in Feb. 2014). These floats have been excluded from the plots in Figure 5A and Figure 5B. For the remaining 14 floats, we think the floats do not need to be corrected for a salinity drift or bias in accordance with the PI's decision. In fact, for these 14 floats, the method should be further tuned either choosing different θ levels to calibrate the float or splitting the float time series when the float sample very different water masses. Among the 14 floats, 7 sampled water off the Spain and Portugal coasts. In these cases, a better choice of the θ levels (above or below the Mediterranean water) reduces the offset in most of the cases. Nevertheless, for the 14 floats, the calibration error is now often larger than 0.01 PSU and the proposed corrections are therefore not significantly different from zero.

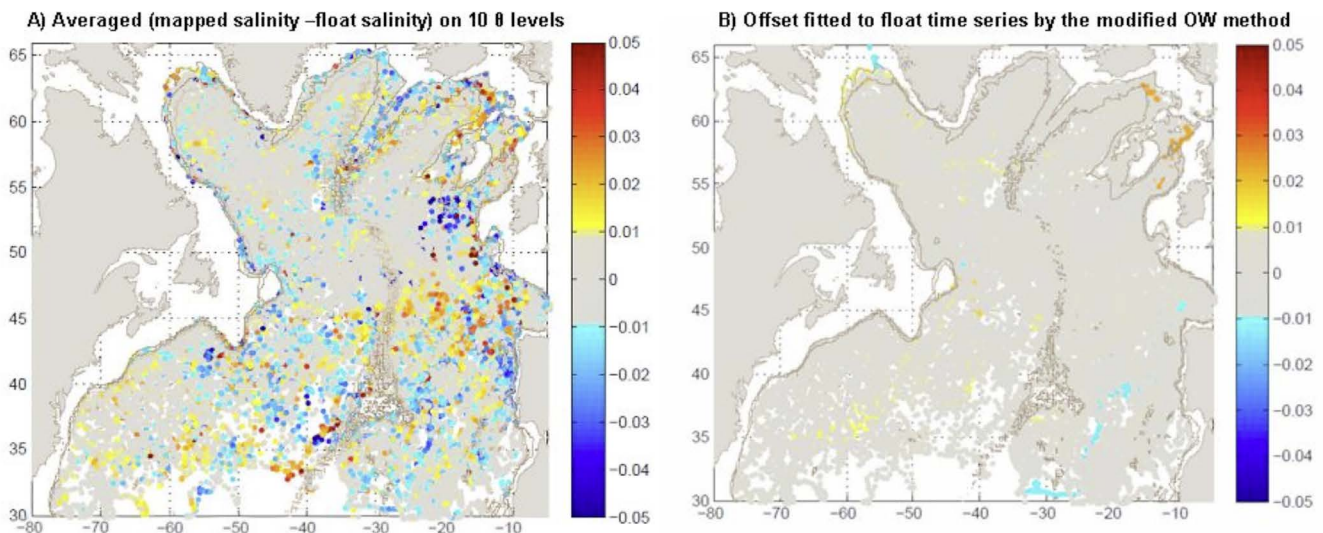
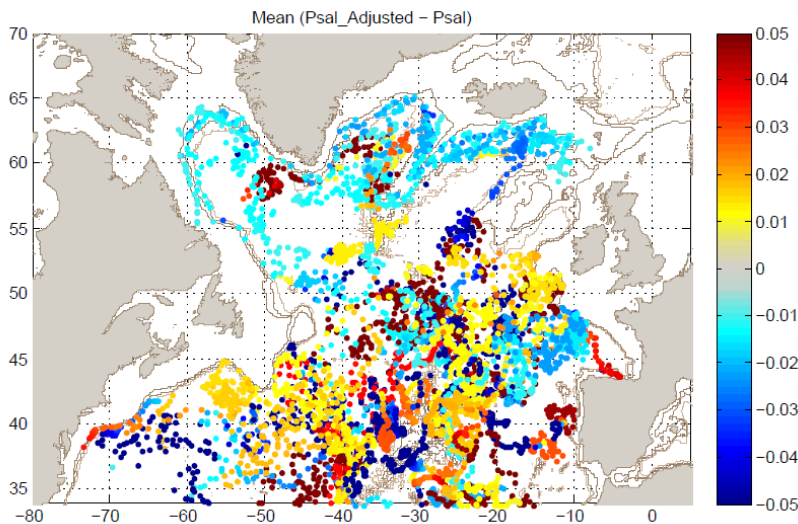


Figure 5: A) Differences (in PSU) between mapped salinities and float salinities averaged over 10 θ levels of a profile. B) Salinity offset (in PSU) fitted to float time series. The modified OW method is used with the ARGO+CTD reference databases.



Finally, we have checked again the corrections of the 186 floats corrected in delayed mode for a salinity offset or drift. Figure 6 shows the delayed mode salinity corrections applied to all the floats in the North Atlantic region.

Figure 6:
Salinity corrections (in PSU) applied on Argo profiles.

Some floats in the subpolar gyre have been corrected for positive salinity biases (i.e. negative corrections) that are comparable to the values shown in Figure 1A. Therefore, we counted 8 floats in this region that may have been over-corrected. These 8 floats have been checked again and new corrections have been made available by mid-2013. Moreover, we have found 22 other floats for which we think it is necessary to revise the delayed mode correction. 12 floats have been checked again by the PI; the correction has been modified and transmitted to the DAC in Feb. 2014. The other floats have not been checked again yet. The full list of these floats can be found on the NA-ARC website.

Ways for improvements of the standard OW method in the South Atlantic-Southern Ocean region

The same approach as in the North Atlantic was followed for the Atlantic sector of the Southern Ocean area (area surrounding the Cape of Good Hope, south of 20°S). We have selected floats that have been processed in delayed mode in this region and for which no salinity bias or drift have been detected according to the PI's decision. Finally, about 420 floats have been selected.

The standard OW method was run for this subset of floats using historical CTD and Argo reference database (note that in this region, the CTD reference database alone is too sparse to give accurate results) as well as the OW method modified in the same way as in the North Atlantic. The fitted offsets to float time series are shown in Figure 7 A and Figure 7 B (standard OW and modified OW method respectively). On average, the modified OW method gives smaller offsets than the standard one. However significant offsets are still found in region of high eddy variability, north of the Sub-Antarctic front and around the Good Hope Cape. If the SAF option is added when selecting the reference profiles, this generally gives offsets closer to zero but only in the region surrounding the SAF. Further improvements of the OW method are then necessary in this region.

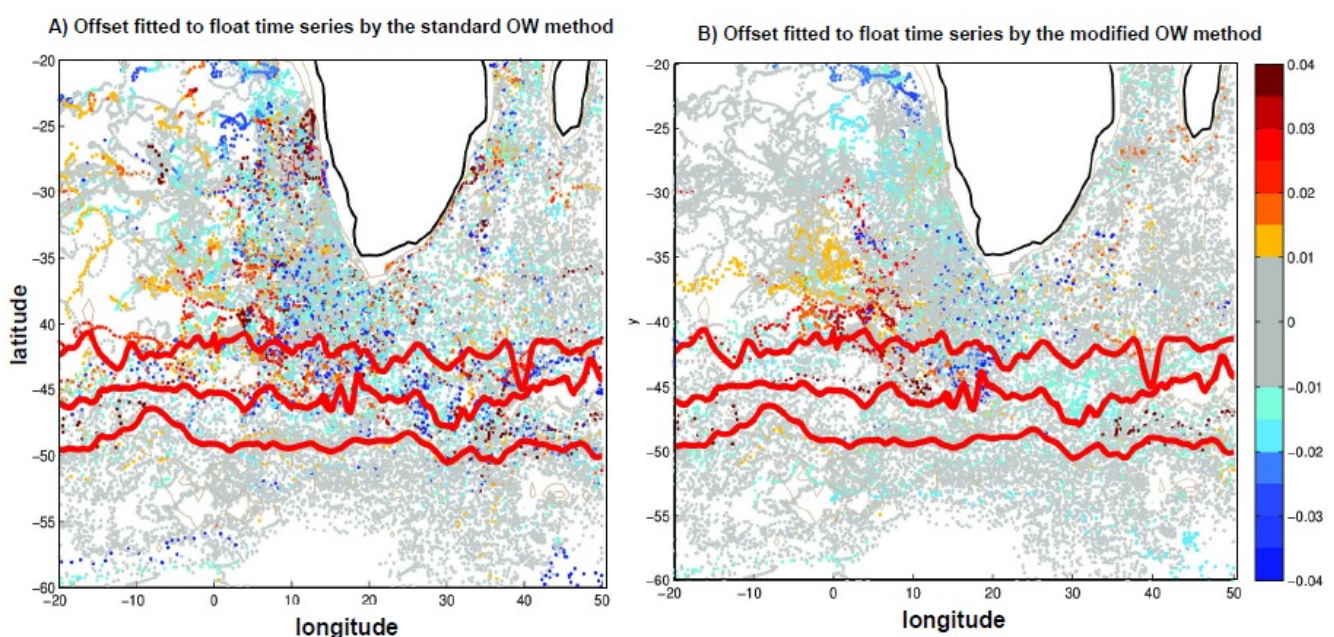


Figure 7: A) Differences (in PSU) between mapped salinities and float salinities averaged over 10 θ levels of a profile for the standard OW method. B) Salinity Offset (in PSU) for the modified OW method as discussed for the North Atlantic. The modified OW method is used with the ARGO+CTD reference databases.

The standard OW method was run for this subset of floats using historical CTD and Argo reference databases (note that in this region, the CTD reference database alone is too sparse to give accurate results) as well as the OW method modified in the same way as in the North Atlantic. The fitted offsets to float time series are shown in Figure 7 A and Figure 7 B (standard OW and modified OW method respectively). On average, the modified OW method gives smaller offsets than the standard one. However significant offsets are still found in region where eddy variability is high, *i.e.*, north of the Sub-Antarctic front and around the Cape of Good Hope. If the SAF option is added when selecting the reference profiles, this generally slightly improve the results but with no sizeable changes because of the high regional variability. Further improvements of the OW method are then necessary in this region.

First of all, we have found that some parameters of the method had to be modified. We have suppressed the parameter that limits the number of reference profiles selected in the first step of the OW method (a maximum of 250 profiles was set in the previous configurations). This prevents the method from randomly selecting reference profiles when the number of historical data (from the area enclosed by an ellipse corresponding to the large spatial scales) exceeds 250. Indeed, the random selection was not found to be suitable in this highly variable environment. We also have reduced the criterion that specifies the vertical box from which historical data are selected for objective mapping. This prevents from using historical data that come from a totally different depth range than the one from the float observed θ -level in this region characterized by weak temperature stratification.

In addition, we have implemented the selection of a reference dataset that has a vertical water-mass structure similar to the one measured by the float (similarly to what is done when the SAF option is selected). To do so, we have chosen to use "the dynamic height" variable as a selection criterion. The dynamic height of the reference profiles is therefore computed and the profiles are retained only if their dynamic height is within ± 2 cm of that of the float profile. Moreover, the reference profiles are selected only if the difference of dynamic height between a 1° gridded climatology and the reference profile is of the same sign as for the Argo profile. This avoids selecting reference profiles in different mesoscale structures such as anticyclonic versus cyclonic eddies or meanders of a front or jet. The dynamic height is added to the covariance matrix of the data in order to attribute more weight to reference profiles with dynamic height close to the float one during the objective mapping stage. In this region an Argo float can sample very different water masses during its drift. This is also an issue for the OW method as the set of θ levels chosen to compare the reference data and the float data is unique along the float path. To overcome this problem, we finally have developed an algorithm to automatically separate the water masses sampled by the float. This is possible by picking up several sets of θ levels along the float path corresponding to the different water masses sampled by the float.

The modified OW method for the Southern Ocean was run for the subset of 420 floats. The results are very encouraging as the offsets fitted to the floats time series are much smaller than those obtained from the previous methods (Figure 8). However further analyses are still needed in order to understand why numerous offsets still exceed the ± 0.01 PSU range. However, in the highly variable region south of Africa, it seems reasonable to correct floats using the modified OW method only when they show a bias or a drift exceeding ± 0.02 PSU.

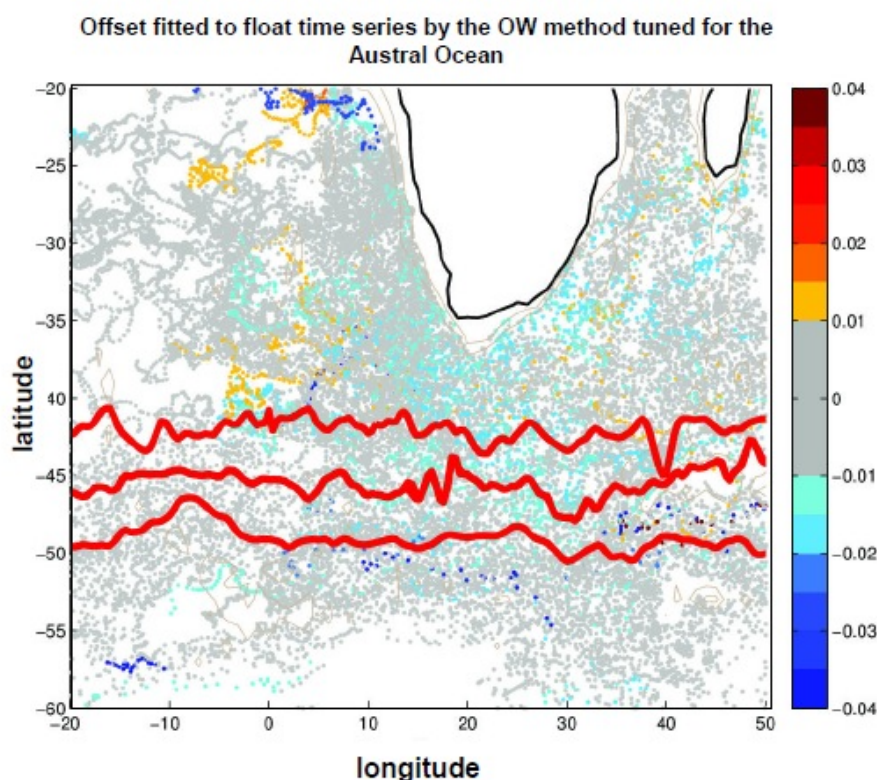


Figure 8: Salinity Offset (in PSU) fitted to float time series for the modified OW method that takes into account the data base and float's profile dynamic heights. The method is used with the ARGO+CTD reference databases.

Conclusions

In this study, we have shown that some modifications of the standard OW method are necessary both in the North Atlantic and the Southern Ocean. These modifications enable PIs to gain confidence in the results proposed by the OW method and make a better decision concerning the need for a salinity correction. In the North Atlantic, we have slightly modified the OW method, introducing a Gaussian decay with a time scale of 2 years when the large scale field is estimated. This better takes into account the large decadal/interannual variability of the large scale salinity field which is assumed to be constant in the standard method. Additional modifications have been implemented for the Southern Ocean area to better take into account the presence of fronts and large eddy variability. Particularly, in this area, we have shown that it is necessary to introduce the dynamic height as an additional constraint when selecting the reference profiles used to calibrate the float data. In the North Atlantic, the modified OW method has been used to check the consistency of the corrections applied on the float salinity data. Overall, we agree with the PI or the Delayed Mode operator of the floats in most of the cases (for about 98% of the floats) when he/she judged that no significant drift or bias was present. Among the floats corrected for a salinity drift or bias by the PIs, we found 30 floats for which the proposed correction differs significantly from our results. For those floats, we think it may be necessary to revise the original correction. It is planned to perform these consistency checks of the North Atlantic floats on a yearly basis. Similar checks will also be conducted in the Southern area.

References

- Böhme, L. and Send, U. 2005. Objective analyses of hydrographic data for referencing profiling float salinities in highly variable environments. *Deep-Sea Res. Part II*, 52:651–664.
- Oka E. and Ando, K., 2004. Stability of temperature and conductivity sensors of Argo profiling floats. *Journal of Oceanography*, 60, 253-258.
- Oka, E., 2005. Long-term sensor drift found in recovered Argo profiling floats. *Journal of Oceanography*, 61, 775-781.
- Owens, W.B. and Wong, A. P. S., 2009. An improved calibration method for the drift of the conductivity sensor on autonomous CTD profiling floats by θ -S climatology. *Deep-Sea Res. Part I*, 56:450–457.
- Sallée, J.B.; Morrow, R. and Speer, K, 2008. Response of the Antarctic Circumpolar Current to Atmospheric Variability. *J. of Climate*, 21,3020-3039
- Sarafanov, A., Sokov, A., Demidov, A. and Falina, A., 2007, Warming and salinification of intermediate and deep waters in the Irminger Sea and Iceland Basin in 1997-2006. *Geophysical Research Letters*, 34, L23609, doi:10.1029/2007GL031074.
- Wong, A.L.S., Johnson, J.M. and Owens, W.B., 2003. Delayed-Mode Calibration of Autonomous CTD Profiling Float Salinity Data by θ -S Climatology. *J. Atmos. and Oceanic Tech.*, 20:308–318.
- Wong, A.L.S, Keeley, R., Carval, T. and the Argo Data Management Team: Argo quality control manual, Version 2.9, 54pp, http://www.argodatamgt.org/content/download/20685/142877/file/argo-quality-control-manual_version2.9.pdf , 2013.

ZONAL JETS AT 1000M IN THE TROPICS OBSERVED FROM ARGO FLOATS' DRIFTS

By **S. Cravatte⁽¹⁾**, **F. Marin⁽¹⁾**, **W. S. Kessler⁽²⁾**

¹IRD/LEGOS, Nouméa, New Calédonia

²PMEL/NOAA, Seattle, USA

Introduction: about the intermediate circulation

The upper circulation of the equatorial oceans has been extensively observed and studied. In particular, the upper circulation of the Pacific Ocean has received much attention for its relation with the El Niño phenomenon. Surface drifters and satellite altimetry gave us a pretty good picture of the mean surface circulation and of its variability. Moorings and repeated hydrographic surveys provided estimates of current velocities across the upper tropical Pacific and Atlantic Oceans, in the first 500 meters or so. In situ observations are sparse below 500 meters, and our knowledge of the oceanic currents in the intermediate and deep equatorial oceans is very limited. However some synoptic deep sections revealed interesting features. Firing (1987) and Firing et al. (1998) first showed evidence in the western Pacific of a series of near-equatorial westward and eastward jets from 3°S to 3°N at intermediate depths, characterized by a large vertical extent, alternating every 1.5°–2° in latitude, with amplitudes of about 10 cm s⁻¹, the so-called “equatorial intermediate current system”. Similar alternating zonal jets have also been evidenced in the equatorial Atlantic Ocean thanks to synoptic sections (Stramma and England, 1999; Boulès et al., 2003), and their zonal coherence along at least 25 degrees in longitude was demonstrated by Ollitraul et al (2006) using acoustic and profiling floats.

Since the advance of the Argo program, and the presence in the global ocean of thousands of autonomous floats drifting at 1000m (or deeper), we now have a new way to observe the intermediate circulation. When compiled, Argo floats' drifts are very valuable tools to determine the absolute velocity at this depth on a global scale. 15 years ago, Firing et al. (1998) noted that “one would like to have a time series of sections covering at least 6°S–6°N, and preferably 10°S–10°N (...) to show whether the pattern of meridionally alternating mean zonal flows continues poleward.” He also noted that “nothing is known about what happens to them at the boundaries”. Argo floats' drifts compilation from 2003 to 2013 offers a sampling density sufficient to resolve the high-resolution meridional structure and zonal extent of the equatorial intermediate current system at 1000m, and makes it possible to answer in part these questions.

Argo float subsurface drift computation, and the ANDRO dataset

Argo profiling floats are originally designed to provide vertical profiles of temperature and salinity every 10 days. They dive to the deepest depth of their profile (usually 2000m), rise to the surface, typically spend a few hours there where satellites determine their position, and dive back to their parking depth (usually 1000m) where they drift for about 9 days before diving again for their next profile. If done carefully, the positions and time of transmissions before and after each dive can be used to compute the subsurface Lagrangian velocities, averaged during the drift period.

We gathered all Argo floats that entered the 12°S–12°N region between 120°E and 70°W, from January 2003 to December 2013, and computed the Lagrangian subsurface velocity corresponding to their drift at their parking depth using their positions and times of transmission. There are several sources of uncertainties on this subsurface velocity computation; the float spends some time at the surface before its first transmission and after its last transmission, during which it drifts with the surface currents; it is also advected by the subsurface currents encountered during its ascent and descent. These errors were estimated and the median error was found to be small (less than 0.5 cm/s). The last important source of error is the parking depth: it is often erroneous in the metafile file (erroneously decoded, or constant even if the float grounded), especially for floats in the Atlantic Ocean. Each float's trajectory and the parameters of its dive were visually inspected to eliminate obvious bad values. Especially, the pressure at the parking depth was computed and inspected carefully. Most of the Argo floats have a parking depth around 1000 m. In the Tropical Pacific Ocean, there are enough floats drifting at 1500m to get a picture of the mean circulation at that depth in some areas, even if large regions remain unsampled. The subsurface velocities at 1000m and 1500m were thus mapped to produce a mean monthly climatological field on a 1° longitude 0.25° latitude grid, using an optimal objective analysis method. The details of the methods used, of the error estimations and of the gridding procedure are described in Cravatte et al. (2012).

Ollitraul and Rannou (2013) recently produced the ANDRO product, a very useful quality-controlled subsurface displacement dataset for the global ocean from all Argo floats till 31 December 2009, with validated parking pressures. We checked that this dataset was consistent with our results in the tropical Pacific.

Mean circulation at 1000m and 1500m in the tropical Pacific

The mean zonal and meridional currents in the Tropical Pacific are shown in Figures 1 and 2. The zonal velocity by far dominates the meridional velocity in most locations, except near the western boundary. Several features stand out:

- a-The zonal velocity at 1000 m is dominated by alternating westward and eastward jets with a meridional scale of 1.5° and speeds about 5 cm/s. Strikingly, these jets are zonally coherent across the entire basin, confirming and extending the synoptic observations of Firing et al. (1998). Moreover, these jets are observed at least from 12°S to 12°N, a wider latitudinal range than shown by previous observations.
- b-The jets are strong in the western and central parts of the basin but weaken and eventually disappear in the east (near 110°W at the equator, farther west poleward).
- c-The jets are stronger in the Southern Hemisphere, where six to seven jets can be identified at 1000 m. They are weaker (except in the west) in the Northern Hemisphere, where seven to eight jets are also identified.
- d- In the western Pacific, the 1000-m zonal jets appear to slant slightly poleward from east to west.

Figure 2 also shows the mean zonal and meridional velocities at 1500m. Even if some regions remain largely unsampled, it gives interesting clues about the deeper extension of the zonal jets. Alternating zonal jets are also present at 1500 m and appear, at first glance, to have a similar geographical distribution than the ones observed at 1000 m. This suggests that the jets have a large vertical extension. It is worth noting that currents at 1500 m are westward along the equator, as at 1000 m. This is surprising, because it is known that, at these depths, equatorial deep jets alternating in the vertical with a wavelength of several hundred meters are present in a narrow equatorial band (Firing et al. 1998, their Fig. 1). Thus, the similarity between 1000m and 1500m zonal currents at the equator is probably coincidental and needs to be further investigated.

Figure 1: Mean zonal currents (upper) and mean meridional currents (lower) (cm/s) at 1000m from optimal interpolation. Topography shallower than 1000-m depth is shaded in dark gray. Updated from Cravatte et al. 2012.

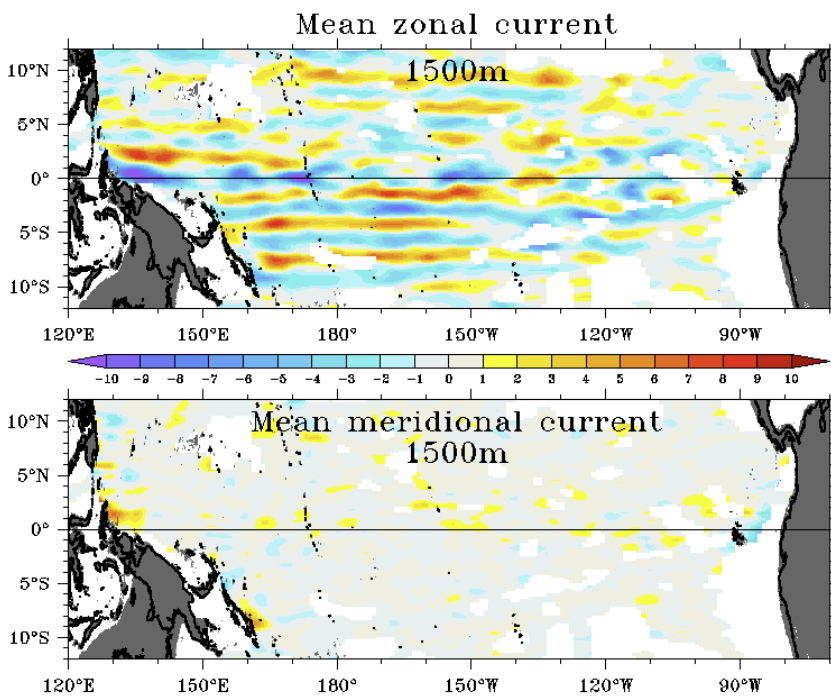
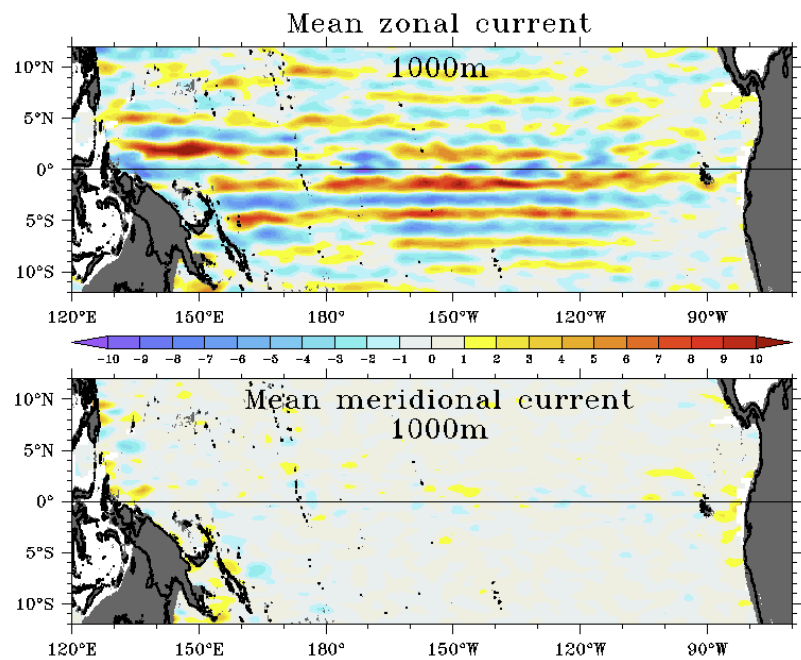


Figure 2: Mean zonal currents (upper) and mean meridional currents (lower) (cm/s) at 1500m from optimal interpolation. Topography shallower than 1000-m depth is shaded in dark gray. Updated from Cravatte et al. 2012.

What happens to them at the boundaries?

Near the western coast of the South Pacific delimited by Solomon Islands chain and Papua New Guinea, the zonal jets originate (or terminate) very close to the coast, and appear to be connected to adjacent westward or eastward jets by meridional velocities (not shown). A northward boundary current is also seen flowing along the Solomon Island chain at 1000m. In the northern Pacific, the situation is analogous, though vigorous eddies dominate the mean circulation, and these recirculations are less clear.

Seasonal variability

It is not possible to resolve the full temporal structure of the jets' variability, given the sampling and the short record spanning only a few years. However, it is possible to characterize their seasonal variability. Figure 3 shows the 1000m zonal velocity anomalies at the equator and at 4°N and 4°S. At the three latitudes, there is a very clear annual cycle of zonal velocity. Current anomalies are out of phase between the equator and 4° and propagate westward at a speed of about 0.43 m/s. This meridional structure and the phase speed correspond to the vertical propagation of the annual Rossby wave described previously based on subsurface temperature changes (e.g. Kessler and McCreary 1993). Interestingly, the zonal currents' seasonal variability exhibits a meridional scale quite different from that of the background mean jets, with a meridional wavelength of 7°–9° instead of 3°. The amplitude of the seasonal variability, which is stronger close to the equator, implies that the most equatorial jets may transiently reverse, as noticed by Gouriou et al. (2006) and explained by Marin et al. (2010). The zonal currents' annual variability is thus superimposed on the mean zonal jets, but the scale difference suggests that the seasonal dynamics are distinct from the background zonal jets' dynamics (Figure 3, middle and right panels).

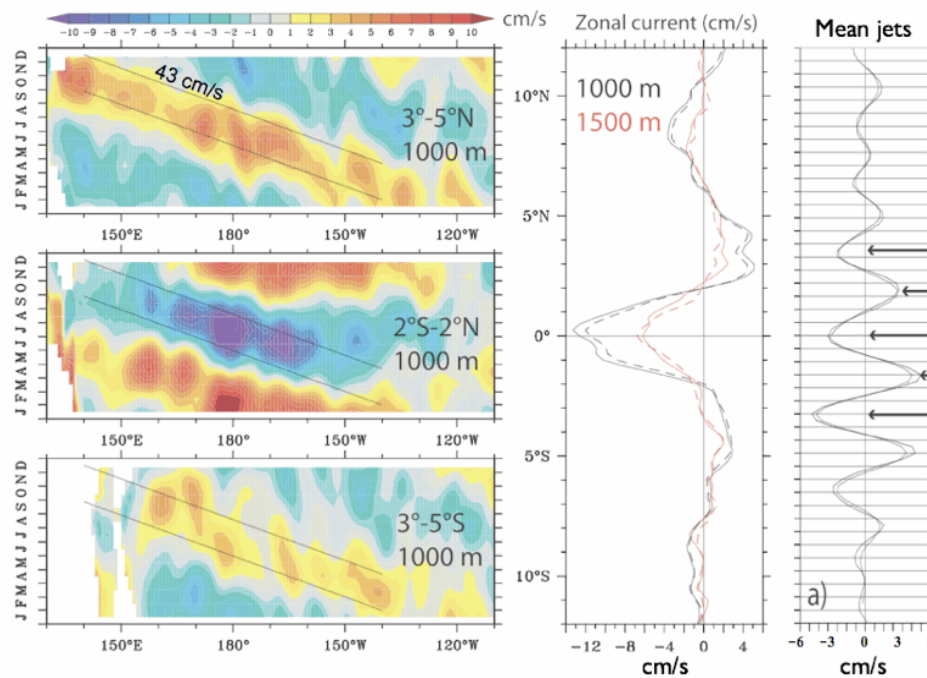


Figure 3: (left) Seasonal anomalies (mean removed) of 1000-m zonal currents (cm/s) averaged between (top) 3°–5°N, (middle) 2°S–2°N, and (bottom) 3°–5°S. (Middle) Zonal velocity anomalies averaged along the paths shown in the left panels (in black lines), between 160°E and 160°W, for 1000-m current anomalies (thin black) and their first annual harmonic (dashed black). The same calculations have been made for zonal current anomalies at 1500-m currents, and 1500-m zonal currents anomalies and their first annual harmonic have been averaged along similar Rossby paths, shifted one month in advance (red thin and dashed lines). (Right) Mean zonal current u at 1000 m in cm/s, zonally averaged in the 160°E–120°W band in the Southern Hemisphere and in the 120°E–120°W band in the Northern Hemisphere. Adapted from Cravatte et al., 2012.

In the tropical Atlantic and Indian Oceans

As in the Pacific, we analyzed the Argo float drifts at 1000m between 12°S and 12°N to characterize the mean velocity and its seasonal variability. We used the ANDRO dataset until December 2009 and updated the subsurface velocities until December 2013. Ubiquitous zonal jets are shown to extend across the tropical Atlantic, in agreement with the findings of Ollitrault et al. (2006) and Ollitrault and Colin de Verdière (2014), but they are weaker than in the Pacific, with larger amplitude in the northern hemisphere. Their meridional scale is about 400km, slightly larger than in the Pacific. They are also weak in the east, and slant poleward in the west. In the Indian Ocean, there are no coherent zonal features emerging from the mean circulation pattern, although the seasonal variability (mainly semiannual) seems to be well resolved (not shown). The mean zonal currents may be hidden by a stronger variability. Understanding the dynamical origin of these differences will be the goal of future studies.

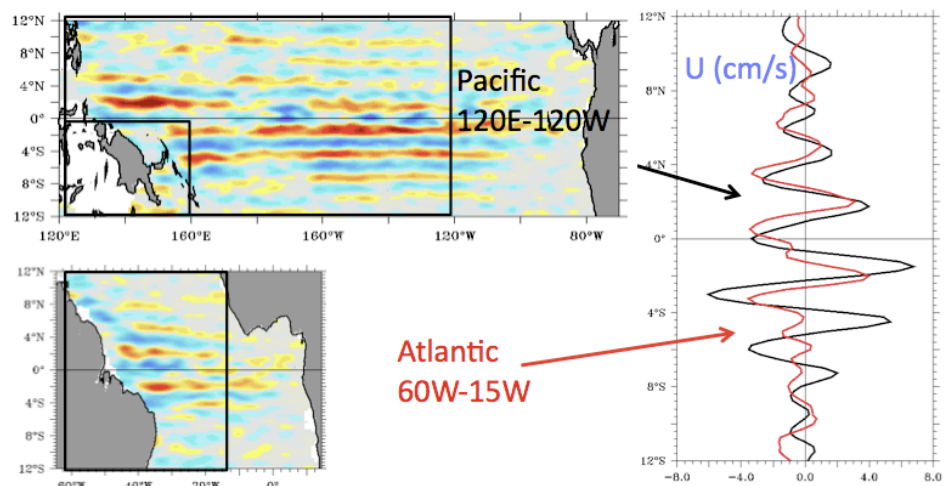


Figure 4: Left: Mean zonal currents from Argo floats drifts (cm/s) at 1000m in the Pacific (upper) and Atlantic Ocean (lower) (cm/s). Right: Mean zonal current at 1000 m in cm/s, zonally averaged in the 160°E–120°W band in the Southern Hemisphere and in the 120°E–120°W band in the Northern Hemisphere in the Pacific, and in the 60°W–15°W band in the Atlantic Ocean.

Conclusion

The analysis of ARGO floats drifts at 1000 m depth indicates that the mean intermediate circulation in the tropical Pacific is dominated by the presence of alternating zonal jets, that had previously only been sporadically observed from synoptic hydrographic cruises at specific longitudes. These jets are coherent over the whole basin width, from Solomon islands to about 2000 km of the American continent, and they are present from 12°S to 12°N. These extra-equatorial jets flow zonally either from West to East, or from East to West, at a speed of about 5-10 cm/s, alternating regularly every 1.5° in latitude. Their hydrological and biogeochemical properties are largely unknown, along with the physical processes responsible for their existence. They are also present in the Atlantic Ocean, but could not be evidenced in the Indian Ocean. Their representation in oceanic models, even at high resolution, is very poor.

The aim of the ZEBRE project funded by LEFE/IMAGO and LEFE/GMMC (PI, S. Cravatte, 2013-2015) is to better document, and understand, the dynamics of these deep extra-equatorial jets in the Pacific ocean and in the other tropical oceans, and to identify their possible link with the deep alternating jets that are observed in the midlatitudes, from the combined analyses of in situ observations (ADCP currents, three-dimensional products of geostrophic velocities, ARGO float drifts) and of numerical simulations. In the context of this project, the CASSIOPEE cruise (2015, PI F. Marin) will acquire a unique set of synoptic in situ observations of the ocean circulation from the surface to the ocean bottom in the Southwest Equatorial Pacific Ocean. The objectives of this cruise are to describe the fine scale meridional and vertical structure of these deep extra-equatorial jets, the hydrological and biogeochemical properties of the water masses they advect, and their possible interaction with the western boundary circulation.

Acknowledgements

This study strongly relies on Argo data subsurface drifts. Argo float data were collected and made freely available by the International Argo Program and the national programs that contribute to it. The Argo Program is part of the Global Ocean Observing System. We would like to thank Michel Ollitrault for his comments and for providing the ANDRO dataset. Many thanks also to Lydia Keppler and Marion Alberty for their careful reading. Sophie Cravatte would also like to thank Cédric Brachet for his support onboard the R/V Thomas G. Thompson during the writing of this note.

References

- Bourlès, B., et al., 2003, The deep currents in the eastern equatorial Atlantic Ocean, *Geophys. Res. Lett.*, 30(5), 8002, doi:10.1029/2002GL015095.
- Cravatte, S., W. S. Kessler, and F. Marin, 2012: Intermediate zonal jets in the tropical Pacific Ocean observed by Argo floats. *J. Phys. Oceanogr.*, 42, 1475–1485.
- Firing, E., 1987: Deep zonal currents in the central equatorial Pacific. *J. Mar. Res.*, 45, 791–812.
- Firing, E. S. E. Wijffels, and P. Hacker, 1998: Equatorial subthermocline currents across the Pacific. *J. Geophys. Res.*, 103 (C10), 21 413–21 423.
- Gouriou, Y., T. Delcroix, and G. Eldin, 2006: Upper and intermediate circulation in the western equatorial Pacific Ocean in October 1999 and April 2000. *Geophys. Res. Lett.*, 33, L10603, doi:10.1029/2006GL025941.
- Kessler, W. S., and J. P. McCreary, 1993: The annual wind-driven Rossby wave in the subthermocline equatorial Pacific. *J. Phys. Oceanogr.*, 23, 1192–1207.
- Marin, F., E. Kestenare, T. Delcroix, F. Durand, S. Cravatte, G. Eldin, and R. Bourdalle-Badie, 2010: Annual reversal of the equatorial intermediate current in the Pacific: Observations and model diagnostics. *J. Phys. Oceanogr.*, 40, 915–933.
- Ollitrault, M., and J. P. Rannou, 2013: ANDRO: An Argo-based deep displacement dataset. *J. Atmos. Oceanic Technol.*, 30, 759–788.
- Ollitrault, M., M. Lankhorst, D. Fratantoni, P. Richardson, and W. Zenk, 2006: Zonal intermediate currents in the equatorial Atlantic Ocean. *Geophys. Res. Lett.*, 33, L05605, doi:10.1029/2005GL025368.
- Ollitrault, M. and A. Colin de Verdière, 2014: The Ocean General Circulation near 1000-m Depth. *J. Phys. Oceanogr.*, 44, 384–409. doi: <http://dx.doi.org/10.1175/JPO-D-13-030.1>
- Stramma, L., and M. England, 1999, On the water masses and mean circulation of the south Atlantic Ocean, *J. Geophys. Res.*, 104(C9), 20,863 – 20,883.

UPPER OCEAN SALINITY STRATIFICATION IN THE TROPICS AS DERIVED FROM N^2 , THE BUOYANCY FREQUENCY

By C. Maes⁽¹⁾, and T. J. O’Kane^(2,3)

¹IRD/LEGOS, Toulouse, France

²CSIRO Marine and Atmospheric research, Hobart, Australia

³ Center for Australian Weather and Climate Research, Melbourne, Australia

Abstract

Using daily vertical profiles of temperature and salinity from an ocean reanalysis over the period 2001-2007, Maes and O’Kane (2014) recently examined the substantial vertical gradients in water properties that occur within the Tropics and the rich variability in the vertical shapes and forms that these structures can assume. Rather than focusing on the strong halocline above the thermocline, commonly referred to as the salinity barrier layer, they specifically took into account the respective thermal and saline dependencies in the Brunt-Väisälä frequency (N^2) in order to isolate the specific role of the salinity stratification in the layers above the main pycnocline. In this letter we provide some further results indicating the impact of a sustained ocean observing network on our ability to resolve the seasonal cycle of salinity stratification by contrasting periods pre- and post-Argo.

Introduction

Several recent reviews and reports of Intergovernmental Panel on Climate Change conclude that there is very little consensus on future changes in El Niño–Southern Oscillation (ENSO), apart from an expectation that ENSO will continue to be a dominant source of year-to-year variability. On interannual to decadal timescales ENSO is arguably the most important part of the world’s climate system. At the heart of this phenomenon is the tropical Pacific Ocean and its response to anthropogenic warming. Focusing on the features relevant to distributions of tuna, Ganachaud et al. (2013) report how projections using a business-as-usual emission scenario would lead to a surface intensified warming in the upper layers and a large expansion of the western tropical Pacific Warm Pool, with most surface waters of the central and western equatorial Pacific reaching temperatures warmer than 29°C by 2100. A substantial freshening of the western Pacific surface waters is also associated with such a warming, increasing *de facto* the stratification of the upper oceanic layers. Although highly uncertain, model simulations of the temperature and salinity characteristics at the eastern edge of the warm pool further indicate the importance of ENSO dynamics and its underlying physical mechanisms (Brown et al. 2014).

Thanks to the increasing number of observations, including satellite observations of the sea surface salinity and in situ profiles collected by the autonomous floats of the Argo network, the zonal displacements of the salinity features along the equatorial Pacific Ocean can now be monitored with accuracy (Qu et al. 2014). According to Maes (2008), it remains important to consider, whenever it is possible, a multi-parameter approach (including direct observations or derived diagnostics such as the Ocean Salinity Stratification (OSS hereafter)) to estimating the salinity stratification thereby removing uncertainties that may result when only one parameter is only considered. This is true especially at the sea surface. At depth, the role of salinity in the static stratification of the ocean upper layers was proposed to identify the predominant role of the ocean salinity stratification within the upper layers. This method takes into account the thermal and the saline dependencies in the Brunt-Väisälä frequency, $N^2(T,S)$, in order to isolate the specific role of the salinity stratification in the layers above the main thermocline.

Recently, following the same idea of a simple partitioning of the thermal and haline effects in the vertical profiles of N^2 , Maes and O’Kane (2014) depict the stabilizing effect of the salinity from the surface down to the main pycnocline, defined as the depth where N^2 is maximum. Their analyses extended to the global subtropical band show that the contribution of the ocean salinity stratification to N^2 is 40-50% of the total (i.e., approximately the same as the thermal contribution) and, in some specific regions, exceeds the thermal part for a few months of the seasonal cycle. These diagnostics are based on vertical profiles issued from a reanalysis modeling effort covering the 2001-2007 period and based on a modified variant of the BODAS ensemble optimal interpolation assimilation system (Oke et al., 2008). Several data sources are considered in such complex systems and are combined optimally in a linear sense to generate a model data synthesis as our best guess of the ocean state at any given time based on the historical observations available. Obviously, the choice of the 2001-2007 period was selected to take into account the increasing (near global) coverage of the Argo data set.

	Period 1994-2000		Period 2001-2007	
	Number of data	Number of platforms	Number of data	Number of platforms
CTD	120977	245	77331	196
Argo profiles	5650	174	380147	4954
XBT	250329	693	204925	534

Table 1: Main sources of temperature and salinity profiles (total number of data and platforms) at the global scales for the (left part) period 1994-2000 and (right part) the period 2001-2007.

In this note, the intention is to underline the importance of the salinity profiles collected by the Argo profilers at the global scales on the OSS seasonal variability. This will be done by comparing some features of OSS computed during two different periods, the original 2001-2007 period as depicted by Maes and O’Kane (2014) and the previous period of 1994-2000. In terms of Argo floats the latter period have documented by 174 profilers giving a little bit more than 5000 profiles (and mainly confined in the Atlantic equatorial sector) as compared to the 350000 profiles and more collected during the 2001-2007 period (see Table 1 for more details). Figure 1 displays the spatial repartition during these periods of time as archived and available through the CORIOLIS DAC. The other sources of observations, including the XBT and CTD for vertical profiles exhibit variations less important in terms of total number of data (Table 1).

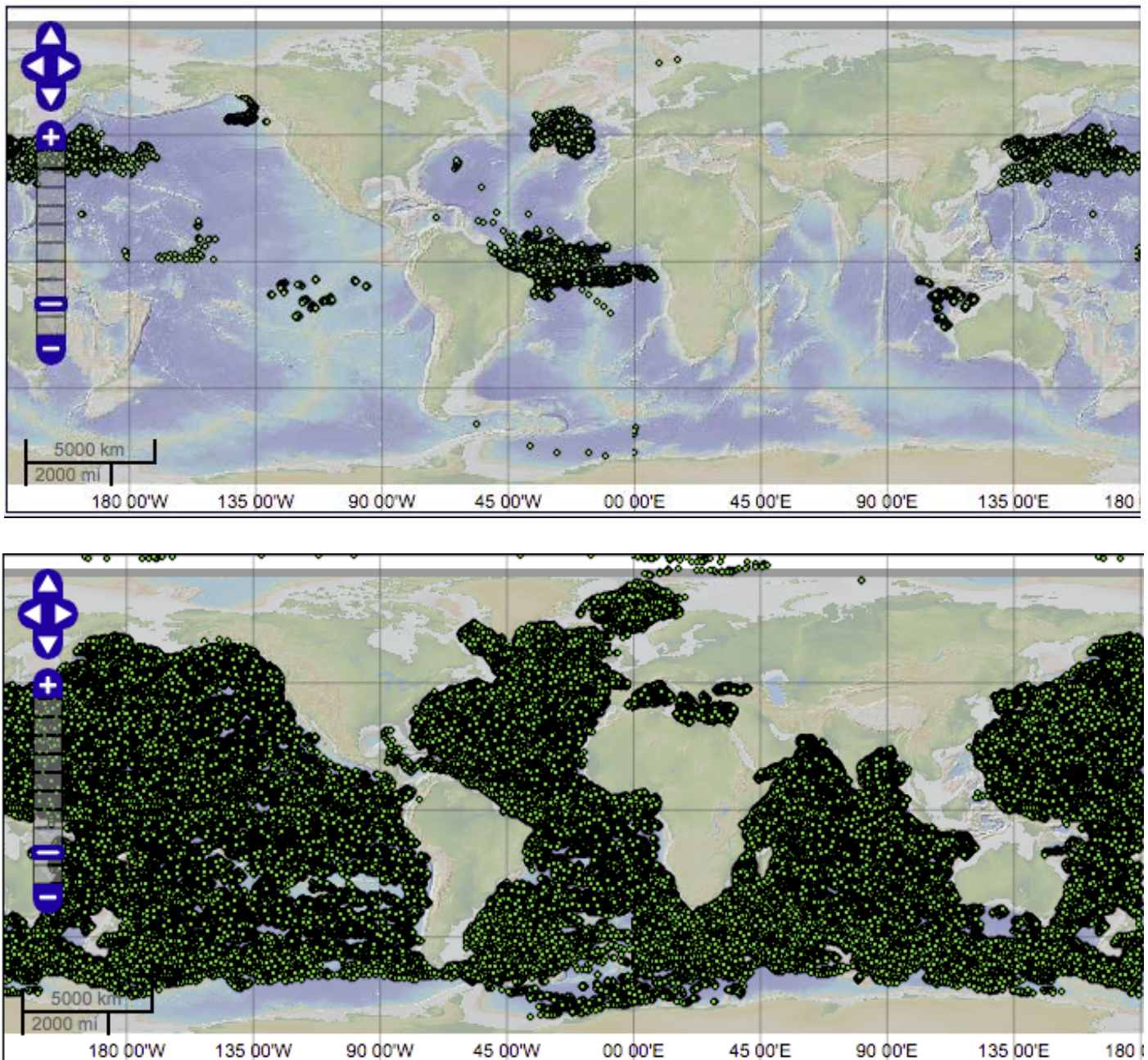


Figure 1: Locations of the full data set of the Argo profiles for the (top) 1994-2000 and the (bottom) 2001-2007 period. The total numbers of each distribution are given in the Table 1. Source: CORIOLIS web site (www.coriolis.eu.org)

Results

The annual mean stratification due to salinity for the 1994-2000 and 2001-2007 periods exhibits roughly the same patterns in the Tropics (Figure 2). Not surprisingly, the magnitude for the previous period is most of the time reduced and this is true especially over all the tropical Pacific Ocean and along the equatorial Indian Ocean. We expect that such differences are due to a better representation of the salinity vertical variability deduced from the observed profiles originating from the Argo floats. In the western equatorial Pacific warm pool, the magnitude is larger by 30-40% for 2001-2007 than for 1994-2000 and the spatial extension of typical values of the OSS larger than 0.2 is greater than 1000 km along the equator. There are also similar variations in the spatial extension in the far eastern part of the basin. This means that if accurate conditions in terms of salinity stratification are required, within the context of ENSO variability, the response of any forecasting systems considering the salinity parameter could be significantly altered by such differences. Conditions of the salinity stratification at the eastern edge of the warm pool during different phases of an ENSO event have been shown to be sensible in a particular coupled atmosphere-ocean model (Maes et al., 2002, 2005). This indicates that the full impact of salinity in ENSO forecasts could be systematically assessed with the most recent network of observations over the last decade and more.

Away from the equator, there are clearly defined regions where the OSS is significantly increased, such as in the Coral Sea or over the Panama warm pool region for instance. In both cases, recent studies reveal that these regions are characterized by strong horizontal fronts that are now observable through satellite missions such as SMOS or Aquarius (Alory et al., 2012; Maes et al., 2013). At the present time, the complex dynamics of the ocean-atmosphere processes involved in the variability of these fronts is not well understood. Our understanding of the latter is limited somehow by errors in estimates of the precipitation fields and by the complexity of the dynamical response of the ocean to atmospheric forcings (wind stress,

interfacial freshwater fluxes, etc...). The main differences in annual mean OSS (Fig. 2) between the respective periods (1994-2000) and (2001-2007) are expected to be due to the increase in the density of observed vertical profiles of salinity over the latter period. It should also be notified that the horizontal gradients of the temperature field at the surface are also increased in association with the salinity front, but the overall thermal effect is less pronounced. Once again, these results plead for sustained efforts to maintain and increase the continuity of collecting salinity observations over the coming decades.

In the Atlantic Ocean, the situation is more difficult to analyze, in part due to the fact that Argo data is available with comparable sampling density during the 1994-2000 & 2001-2007 periods. As noted by Maes and O'Kane (2014) but also reviewed by Reul et al. (2014) in terms of sea surface salinity, the freshwater input through major rivers represents a major source of salinity stratification in the surface layers. However, Figure 2 shows an interesting point: the spatial extension off shore of the OSS in both sides of the Atlantic basin is slightly reduced during the most recent period of time. In the western Atlantic Ocean, Pailler et al. (1999) show that the discharge of the Amazon River plume induces a salinity stratification that covers a large part of the basin in boreal summer-fall. More recently, Coles et al. (2013) document how these plume pathways are highly variable and could influence the dynamical response of the upper ocean layers leading to enhanced eddy stirring and mixing. The salinity seasonal cycle is another very important characteristic that must be considered in such dynamics. In any case, the question of why and how salinity stratification could be enhanced in 1994-2000 as compared to the most recent period remains open. This point deserves more analyses and further work.

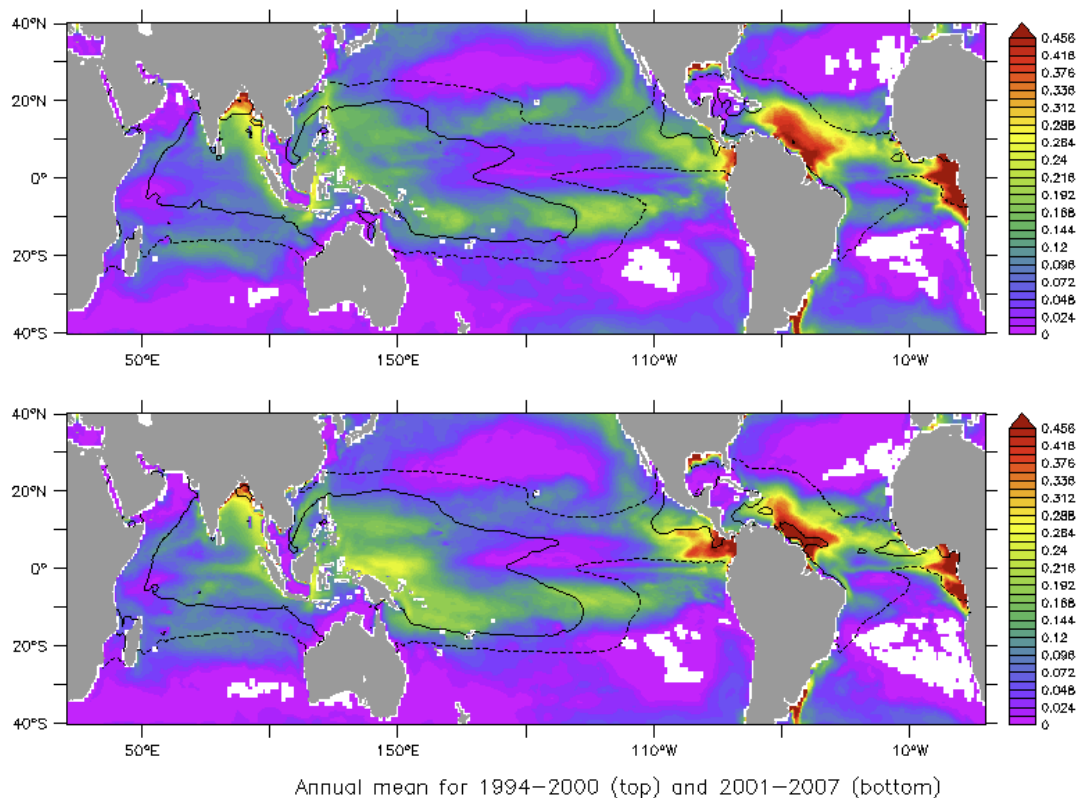


Figure 2: Annual mean OSS (in cph-cycles per hour) for the (top) 1994-2000 and the (bottom) 2001-2007 periods. The black lines represent the 28°C (bold) and 24°C (dash) mean isotherms over the same periods. The regions in white are characterized by the total absence of OSS at the seasonal time scales.

At the scale of the Tropics, the seasonal patterns and variations of the OSS exhibit complex structures that could be exceeded by the thermal counterpart over the same part of the water column during some particular months. The fact that such patterns are mainly characterized by their annual harmonics was shown by Maes and O'Kane (2014). Figure 3 shows that the overall patterns of variability along the equator at the seasonal timescales are not so different between the 1994-2000 and 2001-2007 periods. The relationship of the OSS variations with the 28°C and 24°C isotherms is also included in this figure. In the western Pacific warm pool, it is obvious that the OSS is strongly reinforced during the recent period from the western side of the basin up to the eastern edge of the warm pool and is characterized by a salinity front around 34.8 psu and waters warmer than 29.5°C. This result is consistent with several previous studies focused on the same region and with the most recent analysis of the satellite data (e.g., Bosc et al., 2009; Qu et al., 2014). As a consequence of the results of Figure 3, we believe that the major differences between the two periods are due to the increased availability of salinity profiles during the most recent period of time. This conclusion also prevails for the equatorial Indian Ocean where the semiannual variability along the western coast is harder to resolve from the reanalysis data during the 1994-2000 period. This result indicates that the full impact of the salinity stratification for periods preceding the era of the Argo data should be considered with caution as they could represent only a lower limit of such impact.

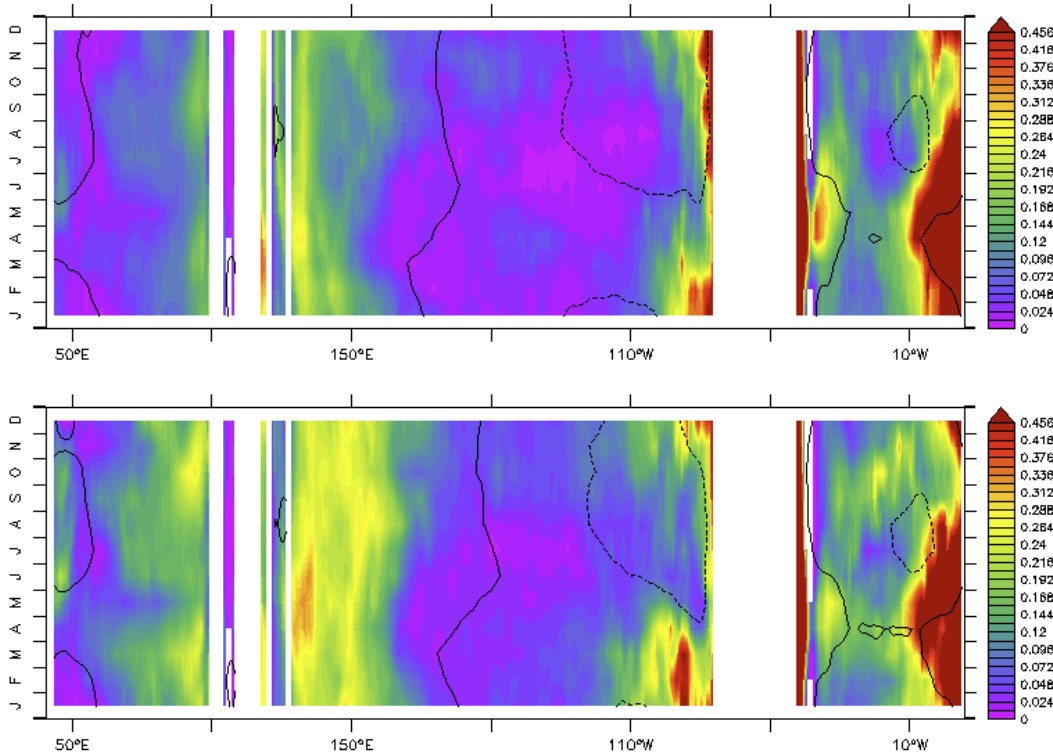


Figure 3: Seasonal hovmuller diagrams along the equator of the OSS (in cph) for the (top) 1994-2000 and the (bottom) 2001-2007 periods. The black lines represent the 28°C (bold) and 24°C (dash) mean isotherms over the same periods.

Despite the potential limitations in the reanalysis data over the early period we nevertheless are confident that the seasonal variations of the sea surface temperature as shown in Figure 3 revealing that the main center of action of the western Pacific warm pool has been moved by more than 10-15° in longitude between the 1994-2000 and the 2001-2007 period are probably robust. Due to the short duration of the period considered in these diagnostics these changes are closely related to the interannual variability of ENSO. It is clear that the early 21st century has been characterized by warm conditions whereas by comparison the end of the 20th century has been a period with several cold periods of La Niña conditions. O’Kane et al. (2013) discuss the role of extra tropical density compensated salinity anomalies on such regimes. The variations of the OSS along the equator for the 2001-2007 period are displayed in the Figure 4. In the Pacific Ocean the strongest signature is associated with the 2006-07 warm event with an evident zonal displacement of the warm pool system toward the central Pacific. The interannual variability is also evident and strong in the Indian Ocean, mainly confined in the eastern side of the basin. How this variability is associated with the local variability or the dipole index, as recently reported from SMOS satellite SSS observations (Durand et al. 2013), needs to be investigated in more detail. In the Atlantic Ocean, where the seasonal variations dominate, there are some significant salinity signals, indicated by large values of the OSS, that seem to appear off shore in the eastern part of the basin, for example the situation in 2006, that deserves closer attention. The analyses of such variations, as well as the identification of the underlying physical processes, are under examination but they are both beyond the scope of the present note.

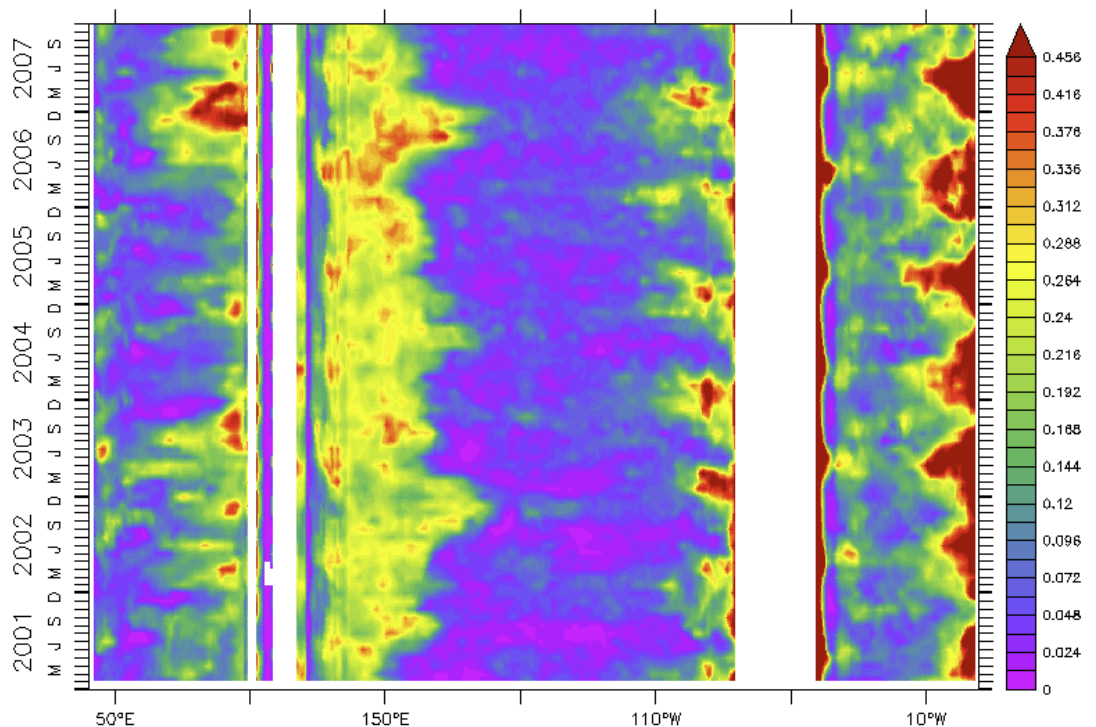


Figure 4: Hovmuller diagram along the equator of the OSS (in cph-cycles per hour) for the 2001-2007 period.

Conclusion

During more than a decade, the key development of the ocean observing system has been the continuous expansion of the Argo float network. Concomitant with temperature profiles, reliable in situ observations of salinity at depth are now available at the global ocean scales. Above the main pycnocline, i.e. at depths lower than 50-250m in the Tropics, Maes and O'Kane (2014) have shown that the stabilizing effect due to salinity could be isolated from its thermal counterpart by separating its role in the computation of the buoyancy frequency. Their analyses are based on the output of a numerical model that assimilates several sources of observations. The seasonal variations are diagnosed and analyzed for the 2001-2007 period when the Argo profiles density began to be important in term of floats number, and spatially homogeneous at the global scales. In the present note this period of time was contrasted with an earlier period where significantly fewer Argo profiles were available (1994-2000) and it has been shown that the two seasonal cycles are characterized by large differences, mainly in terms of magnitude. We believe that these differences are mainly related to the availability of the Argo salinity profiles, even if the interannual variability could play a substantial role during such (short) periods of time. A corollary to this is that caution needs to be applied when undertaking studies and/or experiments that require taking into consideration accurate measures of the stratification due to salinity and in particular when considering periods preceding the era of the Argo data.

Acknowledgements

The Argo data are collected and made freely available by the International Argo Project and the national programs that contribute to it (<http://www.argo.net>). C. M. appreciates the support of an E. Frohlich Fellowship and thanks J. Brown for hosting his recent visit to CSIRO Marine and Atmospheric Research-Hobart in 2013. T. J. O. is funded by an Australian Research Council Future Fellowship and the Australian Climate Change Science Program. Fruitful comments from David Behringer and Nicolas Reul were greatly appreciated.

References

- Alory, G., C. Maes, T. Delcroix, N. Reul, and S. Ilig, Seasonal dynamics of sea surface salinity off Panama: The far Eastern Pacific Fresh Pool, *J. Geophys. Res.*, 117, C04028, doi:10.1029/2011JC007802, 2012.
- Bosc, C., T. Delcroix, and C. Maes, Barrier layer variability in the western Pacific warm pool from 2000 to 2007, *J. Geophys. Res.*, 114, C06023, doi:10.1029/2008JC005187, 2009.
- Brown, J., C. Langlais, and C. Maes, Zonal Structure and Variability of the Western Pacific Dynamic Warm Pool edge in CMIP5, *Clim Dyn*, in press, 2014.
- Coles, V. J., M. T. Brooks, J. Hopkins, M. R. Stukel, P. L. Yager, and R. R. Hood, The pathways and properties of the Amazon River Plume in the tropical North Atlantic Ocean, *J. Geophys. Res. Oceans*, 118, doi:10.1002/2013JC008981, 2013.
- Durand, F, G. Alory, R. Dussin and N. Reul, SMOS reveals the signature of Indian Ocean Dipole events. *Ocean Dyn.*, 63(11-12), 1203-1212. <http://dx.doi.org/10.1007/s10236-013-0660-y>, 2013.
- Ganachaud, A., A. Sen Gupta, J. Brown, K. Evans, C. Maes, L. Muir, and F. Graham, Projected changes in the tropical Pacific Ocean of importance to tuna fisheries, *Climatic Change*, 119:163–179, doi:10.1007/s10584-012-0631-1, 2013.
- Maes, C., B. Dewitte, J. Sudre, V. Garcon, and D. Varillon, Small-scale features of temperature and salinity surface fields in the Coral Sea, *J. Geophys. Res. Oceans*, 118, 5426–5438, doi:10.1002/jgrc.20344, 2013.
- Maes, C. and T. O'Kane, Seasonal variations of the upper ocean salinity stratification in the Tropics, *J. Geophys. Res. Oceans*, 119, 1706-1722, doi:10.1002/2013JC009366, 2014.
- Maes, C., and T. J. O'Kane, Seasonal variations of the upper ocean salinity stratification in the Tropics, *J. Geophys. Res. Oceans*, 119, doi:10.1002/2013JC009366, 2014.
- Maes, C., On the ocean salinity stratification observed at the eastern edge of the equatorial Pacific warm pool, *J. Geophys. Res.*, 113, C03027, doi:10.1029/2007JC004297, 2008.
- Maes C., J. Picaut, and S. Belamari, Importance of salinity barrier layer for the buildup of El Niño. *J. Climate*, 18, 104-118, 2005.
- Maes C., J. Picaut, and S. Belamari, Salinity barrier layer and onset of El Niño in a Pacific coupled model, *Geophysical Research Letters*, 29(24), 2206, doi:10.1029/2002GL016029, 2002.
- O'Kane T., R. Matear, M. Chamberlain and P. Oke, ENSO regimes and the late 1970's climate shift: The role of synoptic weather and South Pacific Ocean spiciness. *J. Comp. Phys.*, <http://dx.doi.org/10.1016/j.jcp.2013.10.058>, 2013.
- Oke, P., G. Brassington, D. Griffin, and A. Schiller, The Bluelink Ocean Data Assimilation System (BODAS), *Ocean Modell.*, 21, 46–70, 2008.
- Paillet, K., B. Bourles, and Y. Gouriou, The barrier layer in the western tropical Atlantic Ocean, *Geophys. Res. Lett.*, 26(14), 2069, doi:10.1029/1999GL900492, 1999.
- Qu, T., Y. T. Song and C. Maes, Sea surface salinity and barrier layer variability in the equatorial Pacific as seen from Aquarius and Argo, *J. Geophys. Res. Oceans*, 119, 15–29, doi:10.1002/2013JC009375, 2014.
- Reul N., S. Fournier, J. Boutin, O. Hernandez, C. Maes, B. Chapron, G. Alory, Y. Quilfen, J. Tenerelli, S. Morisset, Y. Kerr, S. Mecklenburg and S. Delwart, Sea Surface Salinity Observations from Space with SMOS satellite: a new tool to better monitor the marine branch of the water cycle, *Surv in Geophys.*, 35:681–722, doi:10.1007/s10712-013-9244-0, 2014.

MONITORING THE OCEAN WITH TARA – A CORIOLIS PERSPECTIVE

By M. Picheral^(1,2), H. Legoff⁽³⁾, V. Taillandier^(1,2), S. Searson⁽⁴⁾, C. Marec⁽⁵⁾, G. Obolensky^(1,2) and S. Morisset⁽³⁾

¹Sorbonne Universités, UPMC Univ Paris 06, UMR 7093, LOV, Observatoire océanologique, F-06230, Villefranche/mer, France

²CNRS, UMR 7093, LOV, Observatoire océanologique, F-06230, Villefranche/mer, France

³UPMC/LOCEAN, Sorbonne Universités (UPMC, Univ Paris 06)-CNRS-IRD-MNHN, LOCEAN Laboratory, 4 place Jussieu, F-75005, Paris, France

⁴CMORE, Hawaii, USA

⁵Takuvik Joint International Laboratory, Université Laval (Canada) – CNRS (France), Département de Biologie et Québec-Océan, Université Laval, Pavillon Alexandre-Vachon 1045, avenue de la Médecine, Local 2078, G1V 0A6, Canada

Abstract

The Tara Oceans voyage took place on the schooner “Tara” from 2009 to 2013 and visited all oceans to collect samples and data in order to study the relationships between ecosystem biodiversity and function and the physical-chemical oceanographic environment (water mass, transport). The ship was adapted for modern oceanography. Scientific instruments were mounted on a dedicated CTD frame and installed on an underway flow-through system. Data were sent daily to Coriolis and those daily data sent accounted for about half of the oceanographic data sent over the period. Post cruise calibrations were performed leading to a high quality dataset comprising both surface data over a distance of about 60000 nautical miles on all oceans and depth profiles from 700 CTD casts.

Introduction

Tara is a 36m schooner owned by Agnès B. and Etienne Bourgois. The vessel is operated by Tara Expeditions (www.taraexpeditions.org) which conducted two scientific voyages on board between September 2009 to December 2013: Tara Oceans (under the scientific leadership of Eric Karsenti), and Tara Oceans Polar Circle (under the scientific leadership of Eric Karsenti and Chris Bowler) (Karsenti et al. 2011) (Figure 1).

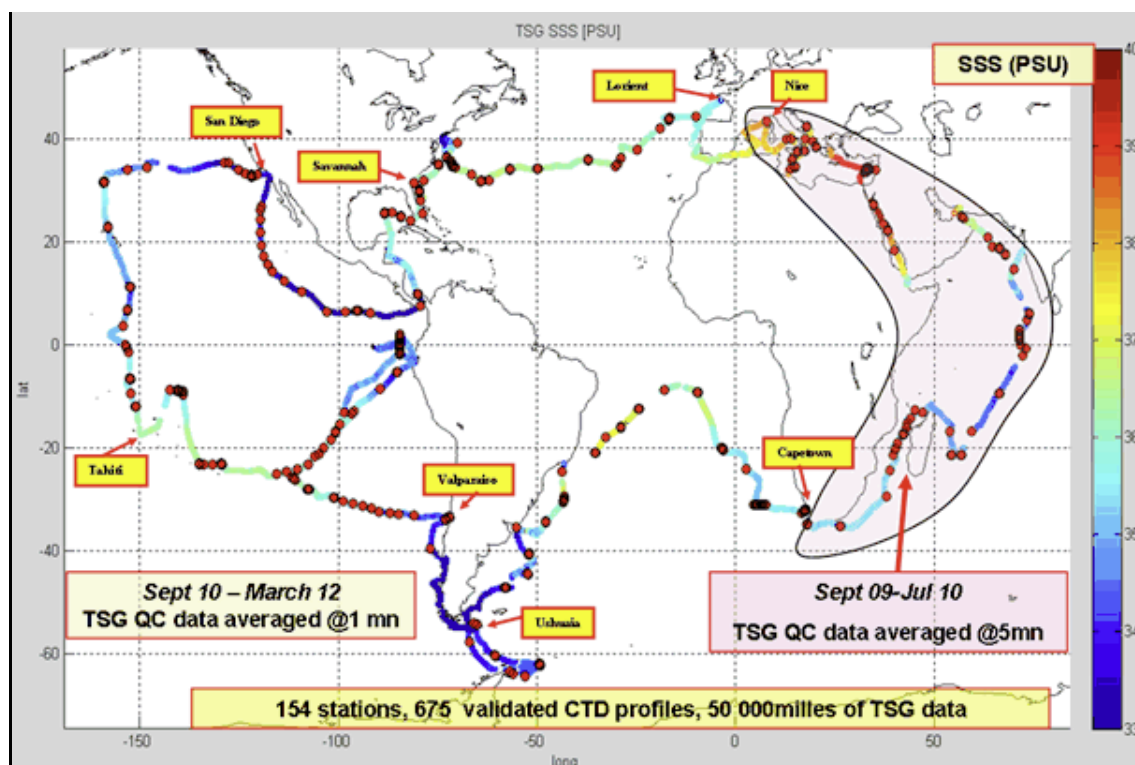


Figure 1: Map of the Tara Oceans Expedition (2009-2012) showing: Sea Surface corrected salinity and position of the 154 stations and main stops

The adapted sailing vessel was specifically equipped with oceanographic instrumentation to measure the physical, bio-optical and chemical characteristics of the upper 1000m and to collect water samples for the whole plankton biodiversity studies (from viruses to fish larvae) using modern imagery and genomic tools.

The emphasis of this article is on the direct measurements and derived parameters that were routinely made as part of the operational oceanographic component. We will present successively the on-board instrumentation, the daily transmissions to Coriolis, the delayed processing mode and finally data validation and distribution processes.

Note that the data from the Polar Circle experiment have not been post processed yet as the voyage was only completed last December 2013. However, the procedures will be similar taking advantage of the experience of the work presented here.

Lexical

The main acronyms used hereafter in this paper are defined here:

- **CTD**: package of conductivity-temperature-pressure probe (the model was a Se-aBird Electronics SBE9 system with additional SBE43 oxygen probe)
- **UVP5**: Underwater vision profiler (developed at LOV)
- **Aquascat**: suspended sediment profiler (could be a turbidimeter or a backscatter system, depending on its model)
- **Biospherical PAR**: cf PAR below. Biospherical is a company.
- **CDOM**: Colored dissolved organic matter
- **HPLC**: High-performance liquid chromatography
- **PAR**: Photo synthetically Active Radiation (usually, refers to radiation between 400 and 700 nm)

On deck equipment

Tara was constructed as an expedition boat. It performed some CTD casts over the past two decades but could not be considered as an oceanographic research vessel. Important modifications of the A frame and winch were thus conducted in collaboration with scientists to allow the deployment of an up to date CTD carousel system and instrumented nets able to go down to 2000m depth. Due to the requirement for a strong 6mm cable that could be used for all instrumentation, the team chose a stainless steel cable without any communication capability. However, an acoustic Scanmar system was added that transmitted the instrument depth to deck in real time.

In order to fit with the limited dimensions of the A-Frame, a specially designed CTD rosette frame (**FIGURE 02a**) was conceived and built for the Tara Oceans project using SeaBirdElectronics components. The system included a 12 bottle (4x12L plus 6x8L) carousel frame from which two bottles were removed. This created space for both the Underwater Vision Profiler (UVP5) and the CTD probe. The Searam which allows the CTD to be run in autonomous mode, is powered by a specially designed Li-Ion battery pack piloted the SBE9 probe, and provides battery to the release mechanisms and all sensors. The UVP5 and the Aquascats had their own internal batteries.

This CTD package included 2 pairs of conductivity and temperature sensors (CT) and a SBE43 oxygen sensor. In addition, a complete set of WETLabs optical sensors were interfaced, including chlorophyll and CDOM fluorometers, a 25 cm transmissiometer and a single wavelength backscatter meter. A SATLANTIC ISUS nitrate sensor and a Hydroptic UVP5 were also integrated. During the Tara Oceans Polar Circle voyage, a second oxygen sensor, a BIOSPHERICAL PAR and a four-frequency Aquascats profiler were added.

The quality of data was maintained and monitored in several ways. Optical sensor data was checked monthly by on-deck and in-situ black offset measurements. CTD profiles were acquired following standard protocols for deployment (that parameterized soaking, lowering and ascending phases of the CTD-Carousel) and for data processing (which included derived environmental quantities such as sensor time lags). Because of space missing on board for storage, no salinity discrete sample was collected during the expedition but the presence of two pairs of CT sensors allowed the continuous cross checking of the quality and stability of these measurements.

Data were all self-recorded at 24Hz and pre-processed as soon as possible after recovery of the instrument package. Surface soak data were removed and the initial quality checks were performed. Customized files were produced and sent daily to Coriolis. They included the following selected parameters only: Pressure, in-situ Temperature, Salinity, chlorophyll Fluorescence and Oxygen.

On board flow through equipment

In addition to the deck equipment, a complex and dedicated flow through system was installed on board before the cruise. This system included various instruments and a water spigot to allow sampling water underway. Instrumentation was not identical during the Tara Oceans and the Polar Circle experiments (**FIGURE 2b**).

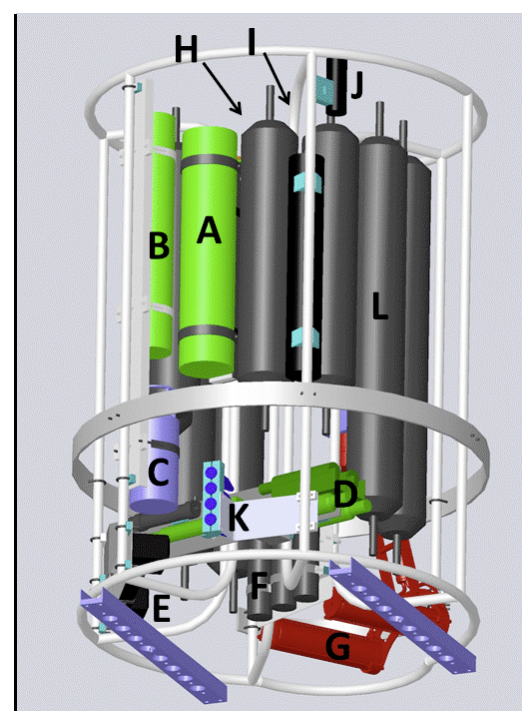


Figure 2a: TARA rosette frame (Polar Circle configuration): A)CTD, B)Searam, C)Battery, D)set of 2 pairs of CT O2 sensors, E)Cstar 25cm transmissiometer, F)CDOM and chlorophyll fluorometers and Backscatter meter G)Underwater Vision Profiler, H)ISUS nitrate sensor, I)Pilon, J)PAR, K)Aquascats transducers and L)Niskin bottles

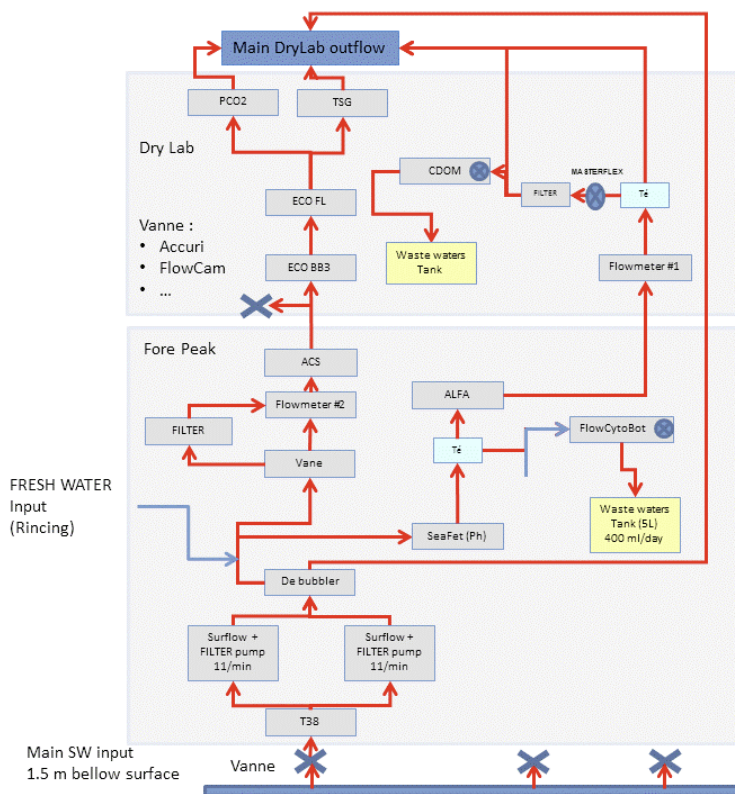


Figure 2b: Flow through schematic (Polar Circle configuration).

The in-line continuous sampling system installed for the Tara Oceans voyage (57,000 miles) included a SeaBirdElectronics (TSG 45 plus T38) temperature and conductivity sensor, a WETLabs AC-S spectrophotometer and a WETLabs chlorophyll fluorometer.

Surface water pumped from ~2m depth was pre-filtered on 0.5 mm stainless steel filter, and temperature at intake measured by the T38 sensor. It was then de-bubbled prior to passing through the spectrophotometer. This section was installed at the front of the vessel. The TSG and chlorophyll fluorometer were located further aft in the Dry Lab. System maintenance (instrument cleaning, flushing) was done approximately once a week for optical sensors and in-between successive legs of no longer than one month for TSG.

During the Tara polar circle expedition additional sensors for pH, PCO₂, Surface PAR (measured on the mast), optical backscattering (3 wavelengths) and fluorescence emission (2 excitation wavelengths) were added to the flow through system (15,000 miles long track) and recorded at 0.1 Hz. Ship attitude, GPS position and Surface PAR were also recorded at 0.5 Hz.

Data files were sent daily to LOCEAN in Paris and forwarded to Coriolis after initial checks were made. During the second part of the voyage, almost all sensors were recorded by a customized Matlab application in a single text file along with ship's GPS position, thus allowing easier post-processing of the data. In addition, these surface temperature, salinity and fluorescence measurements were overlaid on maps to help station selection in conjunction with the prediction models from Mercator Ocean which were received on board via satellite and assembled for sections of the expedition by S. Speich (LPO, Brest) and E.Devred (Takuvik, Quebec).

CTD post-processing (Temperature, Salinity)

The whole dataset has been indexed to international reference scales, accounting for sensor drift measured during routine calibration baths. Results of this assessment are presented hereafter for seawater temperature and salinity. In the absence of other independent data (such as salinity samples), the post-processing task has benefited from (i) two profiles per cast using independent inflows for the CT pairs; (ii) frequent turnover of the sensors to enable regular calibration baths that efficiently kept the accuracy within these international reference scales during the five-years expedition. Differences reported from successive factory calibrations were incorporated supposing linear drifts in time for individual sensors. In practice, time-dependent slope values (and zero offset) for conductivity cells and time-dependent offset values (and unity slope) for temperature probes were computed and inserted into the instrumental configuration file of each cast. The data processing protocol was run again accounting for these static corrections.

Individual sensor drifts (**FIGURE 3, upper panels**) a posteriori revealed an accuracy of the real-time data up to 0.003 degC in temperature and 0.015 PSU in practical salinity. On the other hand, relative misfits between CT pairs (**FIGURE 3, lower panels**) remained of the same order of magnitude thanks to frequent sensor permutations. The nominal accuracy of the post-processed dataset has been assessed considering the agreement between the two estimates: the factory reported values of relative misfits between pairs (shaded areas in upper panels) and the values measured from profiles (red curve in lower panels) appear close by 0.001 degC and 0.005 PSU.

The analysis of the static drifts of CT sensors, whether measured in-situ between independent pairs or individually specified by factory calibration baths, showed well constrained uncertainties of measurement regarding this systematic component. Overall, a nominal accuracy below 0.001 degC for temperature and 0.005 PSU for practical salinity, referenced to respective international scales, has been achieved for the whole dataset of the expedition.

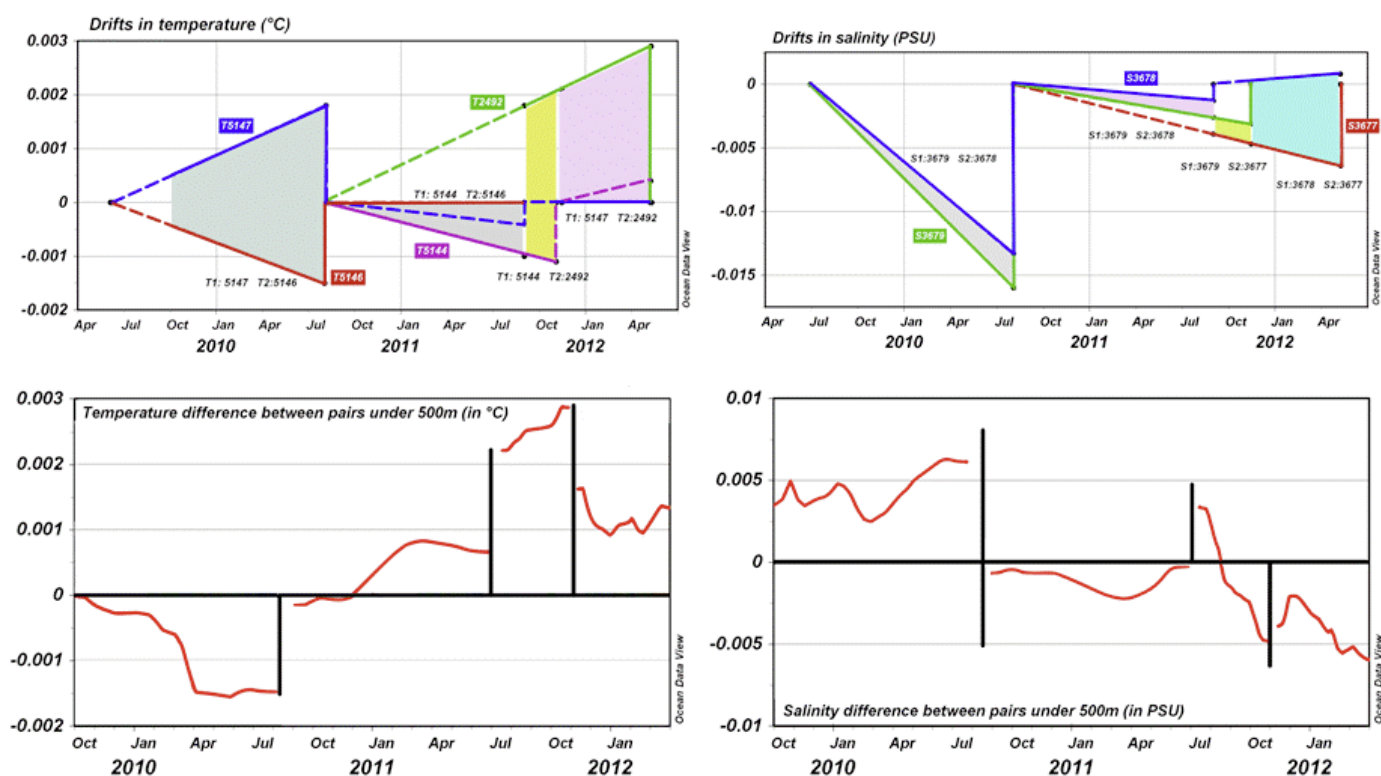


Figure 3: upper panels: drifts of individual TC sensors reported from successive factory calibrations (theoretical drifts between pairs in shaded areas); lower panels: relative drifts between TC pairs (red curves) reported over a wide range of values under 500m.

TSG post processing

T1 and C sensors on SBE45 and T2 sensor on SBE38 have been factory calibrated before departure (05/2009), during the stopover at Cape Town (08/2010) and at the end of expedition (06/2012). Assuming that sensors have been drifting linearly between those calibrations, we applied linear time-interpolations to calibrate the raw TSG data recorded at 0.1 Hz.

Those calibrated data have then been filtered and median averaged every 5 mn for the 1st year (Lorient to Cape Town) and every 1mn for the rest of the cruise (Cape Town to Lorient).

They have been compared to SSS and SST averaged from surface bins of each CTD QC-validated profile (when available above 5dbars) (Table1). For those CTD profiles that were validated as significant for Cross-Comparison (CC), TSG data were corrected (or not) from the (CTD-TSG) differences averaged on stations or group of stations, depending on the type of detected trends or bias. This process produces a set of SST and SSS QC data along 50 000 miles of the whole expedition.

Leg Name	distance [miles]	Valid CTD profiles for CC		(CTD-TSG) SST differences [°C]		(CTD-TSG) SSS differences [PSU]	
		nb	% for leg	median	std deviation	median	std deviation
Lorient to Cape Town	15000	89	58%	0,0042	0,084	-0,00015	0,0185
Cape Town to Ushuaia	7000	82	87%	-0,0001	0,076	0,0001	0,029
Ushuaia to Tahiti	13500	114	58%	-0,0001	0,005	-0,0008	0,01
Tahiti to San Diego	5000	31	43%	-0,0013	0,021	-0,0017	0,003
San Diego to Savannah	4500	51	77%	-0,0001	0,039	-0,0002	0,015
Savannah to Lorient	4500	57	70%	0	0,052	0	0,016

Table 1: (CTD-TSG) differences computed leg by leg on final QC data

As a general conclusion on TSG QC data, (CTD-TSG) median differences on final QC data are always smaller than the sensors initial accuracy (0.002°C and 0.005 PSU), except for SST difference in the central Indian Ocean.

Standard deviations are larger on SST than on SSS. Although the SBE38 temperature sensor was positioned upstream from the pump as close as possible from the seawater intake ($\approx 3\text{m}$ on Tara), the SST signal was randomly biased by the ship's bilge temperature. This is obvious for the first 2 legs (stdv $\approx 0.08^\circ\text{C}$ in Indian Ocean and South Atlantic), and less so afterwards (stdv $< 0.05^\circ\text{C}$). Standard deviations on SSS are smaller than 0.02 PSU except for the South Atlantic leg ($\approx 0.03\text{ PSU}$).

Oxygen and optical sensors post processing

Tara being a small ship, no oxygen sampling could be done on board. The unique SBE43 sensor equipping the CTD was calibrated 5 times and values then checked using the monthly World Ocean Atlas 2009 (Garcia et al. 2009) dataset (**FIGURE 04a**). A careful examination of the data shows that relative differences just before and after factory calibrations do not differ significantly suggesting a satisfactory quality of the dataset.

Optical sensors have been calibrated four times during the project and data and offsets adjusted to deep values when possible. Transmissiometer values were adjusted using a time interpolated reference value and median deep values when available.

Chlorophyll and CDOM fluorescence and backscatter were first corrected using a between-calibration interpolated scale factor and deep measurements as zero.

Chlorophyll fluorescence was then adjusted to chlorophyll a as measured by pigment analysis as follows: all HPLC samples have been compared to median fluorescence measurements at ± 1 m around the Niskin bottle used for HPLC sampling. Negative fluorescence values and total chlorophyll a from HPLC for depth > 200 m and depth < 10 m have been discarded. Only one global conversion between Fluorescence and HPLC was used in order to avoid the creation of an artificial pattern based on local conversion factors between the 2 variables. Values obtained close to the surface have not been corrected for quenching. HPLC can be related to fluorescence by the following exponential function: $\text{FLUO_HPLC} = 1.34 * \text{FLUO_wetlabs}^{0.71}$ (**FIGURE 04b**).

The ISUS nitrate sensor was adjusted to measurements made from NISKIN bottles water samples. A unique adjustment could not be used because of the sensor's drift at the end of the voyage. A station per station local adjustment was performed and propagated to short stations without sampling from the bottles. In order to cover a wide range of nitrate concentrations the adjustment was performed only when more than 5 samples were available and when there was at least one in the deepest half of the profile. The final results are very satisfactory even though the sensor drifted during the last six months of the Tara Oceans expedition (**FIGURE 04c**).

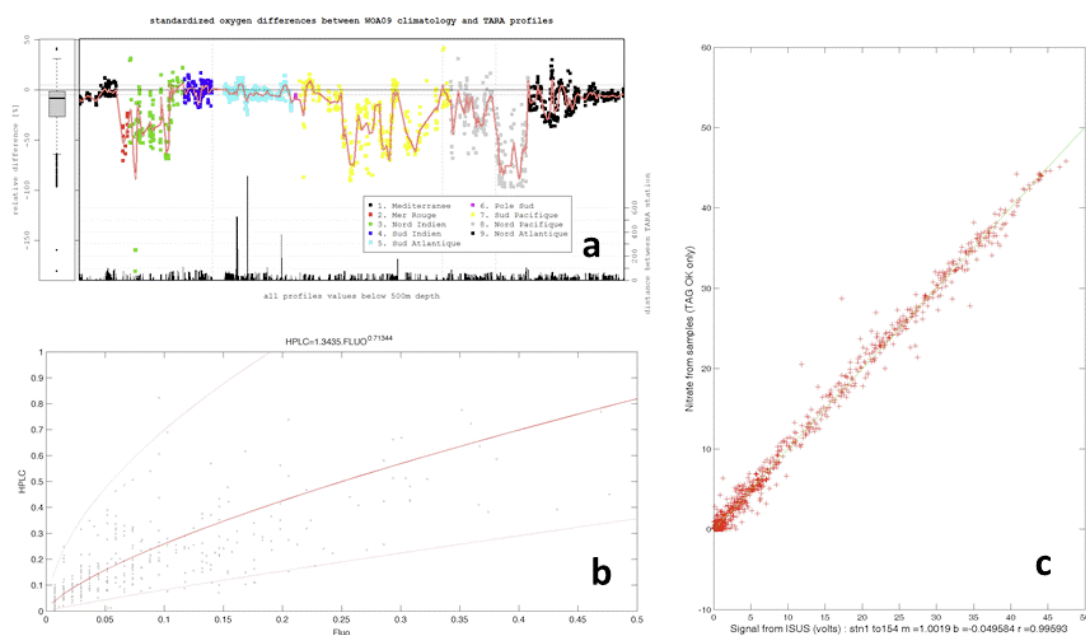


Figure 4: a) Oxygen to climatology adjustment, b) Fluorescence to HPLC adjustment and c) ISUS to nitrate final per station adjustment

Bottle measurements

Due to the limitations of the Searam programming and memory module, standard bottle files could not be processed. A customized Matlab routine was used to calculate CTD measurements from the ascent profiles at the depth where the bottles were programmed to close. Nutrients and carbonate HPLC data obtained from the samples and Large Particulate Matter (LPM) data from the UVP5 were then integrated for these bottles providing a unique database and an Ocean Data View compatible file.

Conclusion

Thanks to the high quality of the equipment installed on board TARA and regular maintenance and calibrations, this effort has led to a unique database of 679 homogenized profiles and 5474 bottles of validated data from the Atlantic (North & South), Mediterranean, Red Sea, Indian Ocean (North & South), Antarctic, Pacific (North & South) and Gulf of Mexico. Data from the Polar Circle voyage (about 160 CTD profiles) will be added later.

The CTD dataset accounted for about half of the data transmitted in real time to Coriolis during the period of the voyage. The broad coverage of the surface TSG and CTD profile datasets can be of great use for the inter comparison made with the ARGO network and other satellite products (SST and SSS) at Coriolis.

The efficient integration of all on deck and flow through sensors on a small 36m ocean class schooner can be considered as a successful workable example for coming expeditions using small research platforms.

Data will be published in Open Access in PANGAEA (May 2014), "Data Publisher for Earth and Environmental Science" (www.pangaea.de).

Acknowledgements

We are keen to thank the commitment of the following people and sponsors who made this unique expedition possible: Etienne Bourgois, the *Tara* schooner and its manager, captain and crew, the CNRS, EMBL, Genoscope/CEA, VIB, Stazione Zoologica Anton Dohrn, UNIMIB, ANR (projects POSEIDON, BIOMARKS, PROMETHEUS, and TARA-GIRUS), FWO, BIO5, Biosphere 2, agnès b., the Veolia Environment Foundation, Region Bretagne, World Courier, Lorient Agglomération, the Foundation EDF Diversiterre, FRB, the Prince Albert II de Monaco Foundation, UNESCO-IOC, Illumina, OCEANOMICS, (ANR au titre du programme "Investissement d'Avenir", ANR-11-BTBR-0008). *Tara* Oceans would not exist without the continuous support of the participating 23 institutes (see <http://oceans.taraexpeditions.org>).

We also thank all the people who helped on board maneuvering the instruments during the long voyage of Tara. Gilles Reverdin supervised the acquisition of TSG data and initiated this work. Nicolas Martin daily checked TSG transmitted files. François Roullier ran the oxygen calibration, Josephine Ras and Léo berline ran HPLC calibration of fluorescence sensors, Pascal Morin supervised nutrients analysis and Emmanuel Boss guided us through the optical sensor data adjustment. Sabrina Speich provided analyses of ocean circulation from altimetry and Mercator Ocean products in order to help in the selection of station sites during some of the legs. Great thanks to Gaby Gorsky and Eric Karsenti who conceived this fantastic scientific project being aware that high quality instruments had to be deployed.

References

Karsenti, Eric, Silvia G. Acinas, Peer Bork, et al. 2011, A Holistic Approach to Marine Eco-Systems Biology. PLoS Biol 9(10): e1001177.

Garcia, H. E., R. A. Locarnini, T. P. Boyer, J. I. Antonov, O. K. Baranova, M. M. Zweng, and D. R. Johnson, 2010. World Ocean Atlas 2009, Volume 3: Dissolved Oxygen, Apparent Oxygen Utilization, and Oxygen Saturation. S. Levitus, Ed. NOAA Atlas NESDIS 70, U.S. Government Printing Office, Washington, D.C., 344 pp.

ELEPHANT SEALS HELP US TO BETTER OBSERVE THE SOUTHERN OCEAN

By **F. Roquet⁽¹⁾**, **S. Blain⁽²⁾**, **C. Guinet⁽³⁾**, **G. Reverdin⁽⁴⁾**

¹MISU, Stockholm, Sweden

²LOMIC Sorbonne Universités (UPMC, Univ Paris 6)/CNRS, Banyuls sur mer, France

³CEBC/CNRS, Chizé, France

⁴LOCEAN Sorbonne Universités (UPMC, Univ Paris 06)-CNRS-IRD-MNHN, LOCEAN Laboratory, 4 place Jussieu, F-75005, Paris, France

Abstract

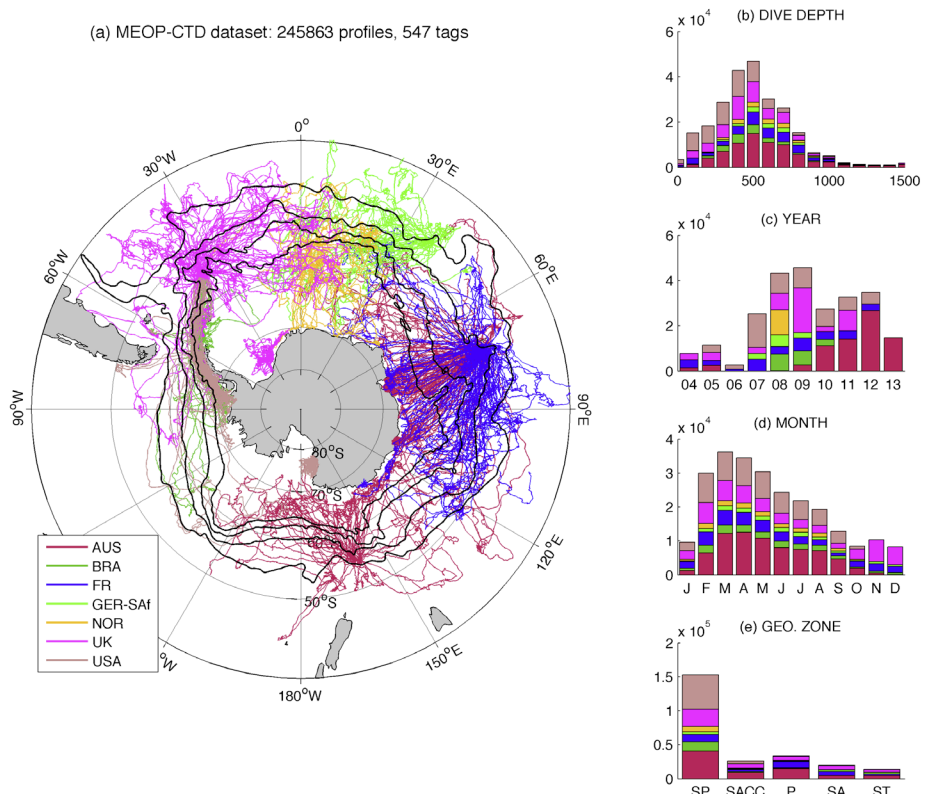
An international team involving researchers from 8 different countries, including French CNRS and MNHN (Museum National d'Histoire Naturelle), have gathered a large number of hydrographic profiles in a wide sector of the Southern Ocean using Antarctic seals equipped with a new generation of oceanographic tags. More recently, fluorescence profiles can also be obtained simultaneously. The Sea Mammal Research Unit in Scotland developed these tags with a strong contribution from the French community, in particular for the optimization of transmitted data compression methods, the quality control of data collected, and the fluorescence sensor. Two new studies published in December 2013 in the journal "Geophysical Research Letters" (Roquet et al., 2013, Blain et al., 2013) demonstrate the importance of the contribution of hydrographic and biogeochemical data collected by these marine mammals, and in particular elephant seals, for the environmental monitoring of the Southern Ocean.

Observing the Southern Ocean

The Southern Ocean plays a fundamental role in regulating the global climate. This ocean also contains a rich and highly productive ecosystem, potentially vulnerable to climate change. Very large national and international efforts are directed towards the modeling of physical oceanographic processes to predict the response of the Southern Ocean to global climate change and the role played by the large-scale ocean climate processes. However, these modeling efforts are greatly limited by the lack of *in situ* measurements, especially at high latitudes and during winter months.

The standard data that are needed to study ocean circulation are vertical profiles of temperature and salinity, from which we can deduce the density of seawater. These are collected with CTD (Conductivity-Temperature-Depth) sensors that are usually deployed on research vessels or, more recently, on autonomous Argo profilers. The use of conventional research vessels to collect these data is very expensive, and does not guarantee access to areas where sea ice is found at the surface of the ocean during the winter months. A recent alternative is the use of autonomous Argo floats. However, this technology is not easy to use in glaciated areas.

In this context, the collection of hydrographic profiles from CTDs mounted on marine mammals is very advantageous. The choice of species, gender or age can be done to selectively obtain data in particularly under-sampled areas such as under the sea ice or on continental shelves. Among marine mammals, elephant seals are particularly interesting. Indeed, they have the particularity to continuously dive to great depths (590 ± 200 m, with maxima around 2000 m) for long durations (average length of a dive 25 ± 15 min, maximum 80 min).



The MEOP-CTD hydrographic database

Profiles of temperature and salinity collected by Antarctic seals, although less accurate than those obtained by Argo profilers or oceanographic vessels, are now the main source of oceanographic data available for the southern part of the Southern Ocean. A unique international collaboration involving German, American, Australian, Brazilian, British, Norwegian, South African and French teams yielded more than 240,000 profiles for the whole Southern Ocean, collected by 550 seals from a dozen different sites in the Antarctic area over the period 2004-2013 (Fig. 1). Data have been edited, corrected, and validated using other in-situ profiles, and are made available to the entire scientific community (T/S accuracy after calibration: $\sim 0.02^\circ\text{C}$ and ~ 0.03 psu respectively). The most critical step in the delayed-mode calibration method consists in removing an offset in salinity (typically ± 0.1 psu) introduced by an external-field effect on the inductive coils of the conductivity sensor.

As part of a first study assessing objectively the contribution of seal-derived data in the observation of the Southern Ocean (Roquet et al., 2013), we used the ECCO (Estimating the Circulation and Climate of the Ocean) state estimation framework (Wunsch and Heimbach, 2013). State estimation consists in producing a least-squares fit of a global ocean circulation model to a given set of observations. This method is computing intensive, but it has the advantage of producing a dynamically consistent description of the time-varying distribution of physical ocean properties (currents, temperature and salinity), which is as consistent as possible with observations. The ECCO framework is mainly used to produce dynamically consistent syntheses of most existing data (both in situ and satellite) during the 1992-present period (products available at <http://ecco-group.org>). Here, we compared two state estimation experiments, both constrained with Argo profiler data, but differing in the use or not of seal-derived data as a constraint.

It was found that including seal-derived data substantially modifies the estimated surface mixed-layer properties and circulation patterns within and south of the Antarctic Circumpolar Current. In particular, a decrease in surface temperatures near the Antarctic continent and a substantial increase in salinity west of the Antarctic Peninsula were found in the seal-constrained estimate. These differences were linked to changes in the behavior and extent of the estimated sea ice cover, with an overall increase of 10% in sea-ice extent (Fig. 2). Agreement with independent satellite observations of sea-ice concentration was improved, especially along the East Antarctic shelf where there is a large concentration of seal data.

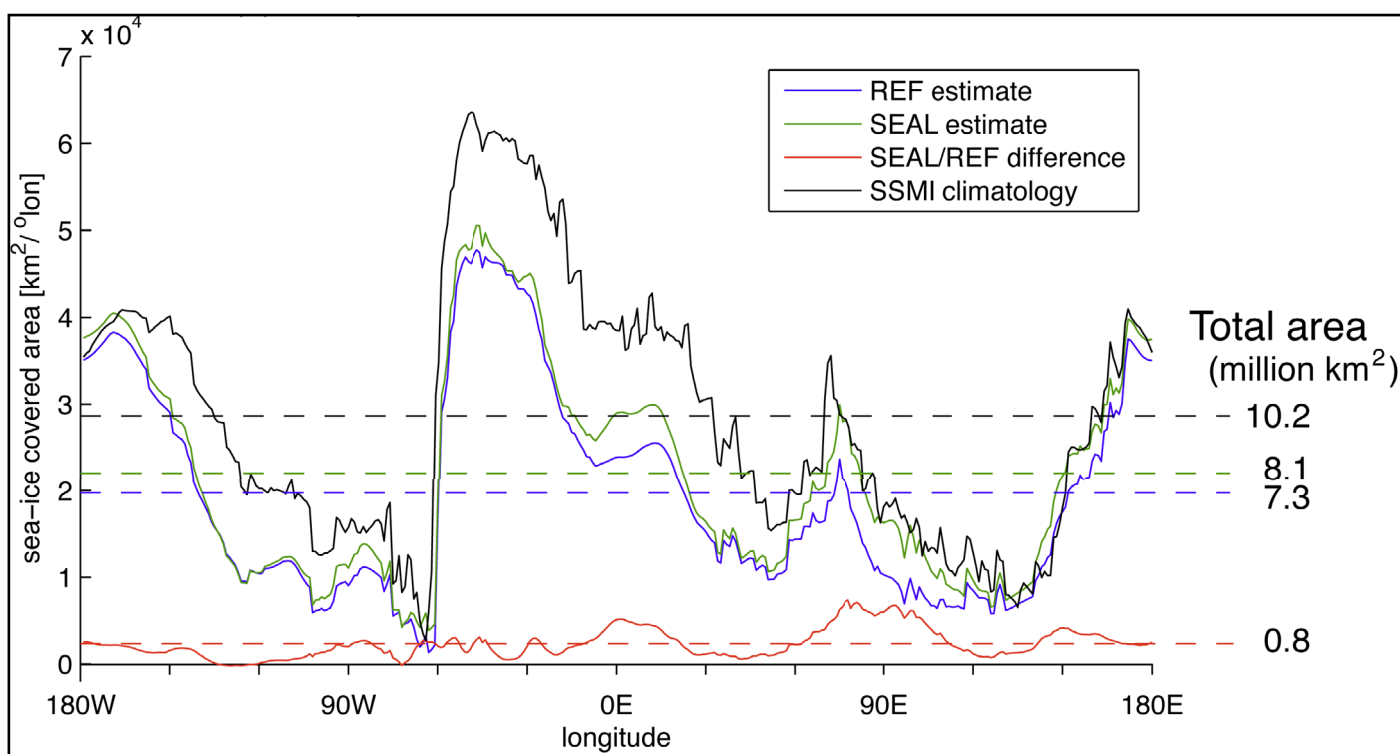


Fig 2: Distribution of annual-mean zonal integrals of sea-ice concentration, for the two state estimates: REF is a state estimate constrained by Argo data only, while SEAL is constrained by both Argo and seal data. A climatology of SSM/I satellite observations is superimposed, showing that the SEAL state estimate is still featuring a deficit in sea-ice cover relative to observations, although significantly reduced as compared to the REF state estimate (adapted from Roquet et al., 2013).

Sampling chlorophyll distribution with instrumented seals

As part of the IPSOS-SEAL project, 23 elephant seals from the Kerguelen Islands were also equipped with Argos CTD combined with a Cyclops 7 fluorometer (Turner design) over a three years period starting in 2007, allowing the collection of over 2000 temperature/salinity/fluorescence profiles sampling nearly all months of the year. In parallel, the analysis of fluorescence data allowed a team of researchers from the Laboratoire d'Océanographie Microbienne (LOMIC, Banyuls-UPMC-CNRS), Laboratoire Océanographique de Villefranche Sur Mer (UPMC-CNRS) and Centre d'Etudes Biologiques de Chizé (ULR-CNRS) to construct for the first time a climatology of the mixed layer depth and the amount of chlorophyll that it contains which led to two important discoveries (Blain et al., 2013, see also Fig. 3). Blain et al. (2013) found that light conditions in the Southern Ocean are favorable for the development of phytoplankton over a long period ranging from October to April. This result is surprising because it shows that the presence of very deep mixed layer found in these regions (often exceeding 100 m) does not prevent photosynthesis from taking place. However, it also appeared that the maximum amount of chlorophyll that can be accumulated in the mixed layer was in fact controlled by the phytoplankton itself, due to self-shading by phytoplankton. The strong link between light availability and phytoplankton being now quantified, this work should help in predicting the response of phytoplankton to ongoing climate change in the Southern Ocean.

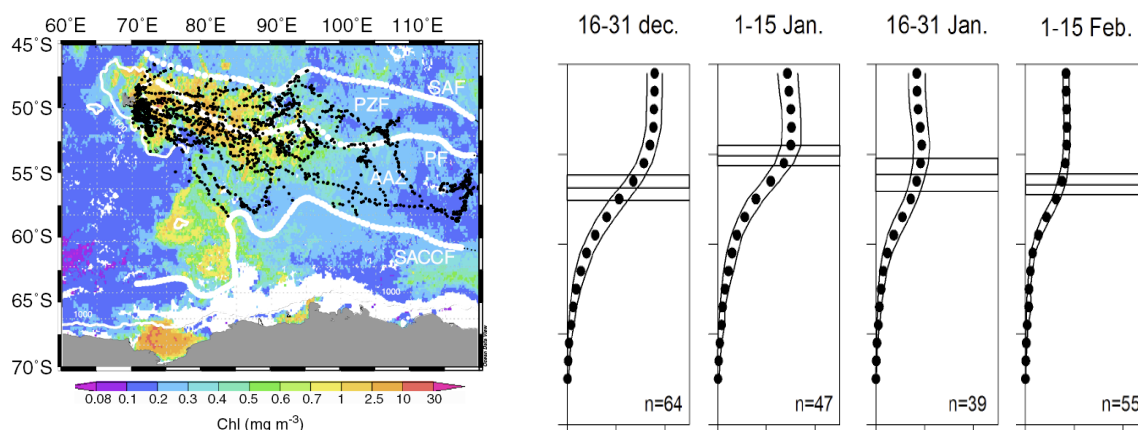


Figure 3: (left) Map of the study area, superimposed on satellite observations of surface chlorophyll concentrations from December 2009. The area delimited by the Sub Antarctic Front and the South Antarctic Circumpolar Current Front (SACCF) corresponds to an iron-fertilized region. (right) Associated bi-monthly climatology of Chl_a for the peak bloom period, with the mean (\pm SE) mixed layer water depth indicated with the gray line

Conclusion

Instrumented seals have now demonstrated their ability to collect data in places where access is difficult, if not impossible, offering an attractive and original interdisciplinary approach that benefits both biologists and climatologists. A growing number of studies focus on the Southern Ocean mainly because of issues related to climate change and the importance of the ocean in large global climate balance. In this context the contribution of these data is of particular interest to the scientific community with a potential that remains largely unexplored.

The SO-MEMO now constitutes a significant part of the French contribution to the observation of the Southern Ocean. The French seal data can be obtained on demand at the Coriolis Oceanographic Data Centre (www.coriolis.eu.org). The larger MEOP-CTD dataset can also be obtained on demand (contact directly the authors). Hydrographic seal data are already incorporated in the Coriolis CORA database, and they are being used to produce GLORYS reanalysis (joint project Mercator Ocean/CNRS/Coriolis/CLS). They are also used to produce the ISAS climatological product (LPO/CNRS, Brest). Data are available both in real time and delayed time through CORIOLIS. Real time data are mostly provided to CORIOLIS on order to be assimilated in operational models such as MERCATOR OCEAN.

Acknowledgements

The French contribution of this international study was carried out as part of activities of the French observatory MEMO (Mammifères Echantillonneurs du Milieu Marin), funded by the two CNRS institutes INSU and INEE. The project benefited from the financial and logistic support from CNES (TOSCA program), the Institut Paul-Emile Victor (IPEV), the Total Foundation and the ANR. MEMO is closely associated to the Coriolis centre, which distributes real-time and delayed-mode products, and is part of the SOERE consortium CTD02 (Coriolis-temps différé Observations Océaniques, PI: G. Reverdin).

References

- Blain, S., S. Renaut, X. Xiaogang, H. Claustre, and C. Guinet (2013). Seasonality in chlorophyll and light-mixing regime in the iron fertilized Southern Ocean, *Geophysical Research Letters*, DOI: 10.1002/2013GL058065
- Roquet, F., C. Wunsch, G. Forget, P. Heimbach, C. Guinet, G. Reverdin, J.-B. Charrassin, F. Bailleul, D. P. Costa, L. A. Huckstadt, K. T. Goetz, K. M. Kovacs, C. Lydersen, M. Biuw, O. A. Nøst, H. Bornemann, J. Ploetz, M. N. Bester, T. McIntyre, M. C. Muelbert, M. A. Hindell, C. R. McMahon, G. Williams, R. Harcourt, I. C. Field, L. Chafik, K. W. Nicholls, L. Boehme, and M. A. Fedak (2013). Estimates of the Southern Ocean General Circulation Improved by Animal-Borne Instruments. *Geophysical Research Letters*, 2013GL058304.
- Wunsch, C. and P. Heimbach (2013). Dynamically and kinematically consistent global ocean circulation and ice state estimates. In: G. Siedler, J. Church, J. Gould and S. Griffies (eds.): *Ocean circulation and climate*, Chapter 21, pp. 553–579, Elsevier.

Observing System experiment: A simple tool to assess the multiple roles played by ARGO observations on the operational forecasting system of mercator ocean.

By V. Turpin⁽¹⁾, E. Remy⁽¹⁾, P-Y Le Traon⁽²⁾

¹ MERCATOR OCEAN, Toulouse, France

² IFREMER & MERCATOR OCEAN , Toulouse, France

Abstract

OSEs (Observing System Experiments) are a useful tool to understand the functioning of the data assimilation system and to quantify the impact of observations on ocean analyses and forecasts. In the framework of E-AIMS project (<http://www.euro-argo.eu/EU-Projects-Contribution/E-AIMS>), a series of OSEs have been performed in order to assess the impact of Argo observations on the Mercator Océan global analysis and forecasting system at $\frac{1}{4}$ degree resolution. This paper provides with a brief summary of results and highlights the unique contribution of Argo for operational oceanography.

Introduction

Ocean Forecasters from Mercator Océan need to provide Observing system agencies with the assessment of the role of each specific observing system in the performance of their data assimilation system. Observing system agencies need this information in order to make sound decisions on long-term investments for the future ocean observing systems. On the one hand, from a political point of view, it is necessary to quantify the improvement made by an observing system such as Argo, moorings or altimetry for example in order to decide on long-term investments. This also requires that scientists make their assessment understandable to non scientific decision-makers. On the other hand, from a scientific point of view, it raises the issue of how to reduce such complex system of systems into a few indexes in order to explain the necessity of a particular data-type.

This paper will give examples of results from Argo OSE highlighting the role played by this observing system on the overall performance of the Mercator Ocean global forecasting system. Note that this paper is built from an operational oceanography point of view and it is important to warn that the conclusions might be different from other perspectives (e.g. climate). It should be seen as a non-exhaustive series of examples that assess the importance of Argo data assimilation.

The 4 OSEs performed over the year 2012 in order to assess the importance of Argo temperature (T) and salinity (S) profiles in the Mercator Ocean $\frac{1}{4}$ degree operational system (PSY3) are described in the next section. It is important to remind that results from OSEs are totally dependent on the analysis system used and on the parameterization of the assimilation scheme. The conclusions might differ in other configurations.

Tools and method

Analysis system

In this study, we used the Mercator Océan operational ocean forecasting system (here after called PSY3, [Lellouche et al., 2012](#)). It is a $\frac{1}{4}$ degree global ocean grid discretized on 50 vertical levels that decrease from 1m resolution at the surface to 450m at the bottom of the sea. The model used is NEMO 3.1. The assimilation system has been developed at Mercator Océan. It cycles on a 7 day window and relies on a reduced order Kalman filter (SEEK) ([Pham et al., 1998](#)) with 3-D multivariate modal decomposition of the forecast error.

The 2012 assimilated observations consist on 4 along track SLA altimeter data (Envisat, Jason1, Jason2, Cryosat) from MyOcean Sea Level TAC. The mean dynamic topography (MDT) named "CNES-CLS09" derived from observations is used as a reference for SLA assimilation. SST with a $\frac{1}{4}$ ° resolution comes from NCEP and NOAA and includes AVHRR and AMSRE observations ([Reynolds et al., 2007](#)). Temperature and salinity profiles from MyOcean InSitu TAC ([Cabanes et al., 2013](#)) are also assimilated. Table 1 gathers the PSY3 characteristics.

System Name	Resolution	Model	Assimilation	Assimilated observations
PSY3	Horizontal: $\frac{1}{4}$ ° Vertical: 50 levels	ORCA025, NEMO 3.1, LIM2 EVP, Bulk CORE, 3h atmospheric forcing (ECMWF)	SAM (SEEK) IAU 3-D Var bias correction	"AVHRR+AMSRE" SST SLA T/S vertical profiles

Table 1 : Characteristics of the Mercator Océan PSY3V3R3 system

Observing System experiment: A simple tool to assess the multiple roles played by ARGO observations on the operational forecasting system of mercator ocean

In-situ Observing System

The 2012 in-situ dataset (figure 1) is extracted from the Coriolis database developed by the research and development team of the French program Coriolis. Argo floats provide with measurements of temperature and salinity from the surface to 2000 meter depth every 10 days in each basin of the globe. More than 3000 floats drifted in 2012 over the global ocean, with less than 3° mean spacing. Other than Argo Insitu data (called "other Non Argo Insitu data" hereafter) are also available: XBTs provide with temperature measurements mostly along the main ships routes from surface to 800 meter depth. The XBT network is irregular in time and space but gives a good vertical resolution of the sampled layer. Moorings are mostly in the tropical oceans and consist of TAO/TRITON moorings in the Pacific, PIRATA in the Atlantic and RAMA in the Indian Ocean. Typically, buoys sample the ocean from surface to 500m or 750 meter depth at 10 to 15 levels. Other moorings are sampling in specific region such as the strait of Drake or the Labrador Sea. Sea mammal's CTDs are localized in specific region of the high latitude ocean as the Svalbard islands, the "French Southern & Antarctic Lands" and the Ross sea. In those regions in 2012, CTDs from Sea mammals are the first observing system available. Gliders are set up to sample temperature and salinity from surface to paring depth and in a specific area.

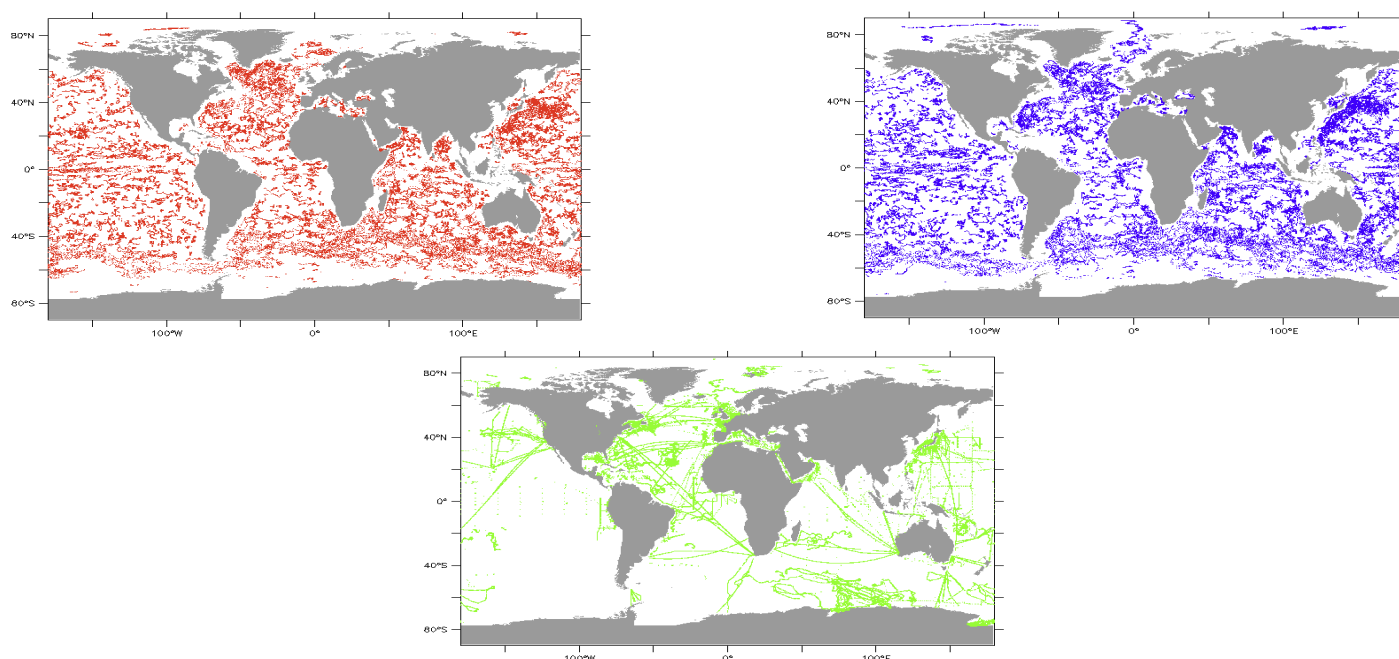


Figure 1 : Spatial distribution of 2012 insitu dataset divided in 3 sub datasets. 1a) "odds" argo profiles, 1b) "evens" argo profiles, 1c) other insitu observations.

Experiment design

The OSEs presented here focus on the impact of the Argo observing system on T and S estimation. Four experiments have been performed from the year 2012 which corresponds to 50 analyses cycles of 7days. In the 3 first experiments, altimetry and SST data are systematically assimilated by the PSY3 system. The difference in the 3 experiments resides in the data assimilation of Insitu data.

- The first reference experiment is named **Run-Op**. SLA, SST and all In-situ data (Argo + "other Non Argo insitu data") are assimilated.
- In the second experiment, named **Run-Argo2** hereafter, SLA, SST, 50% of the Argo data and all the "other Non Argo Insitu data" are assimilated.
- In the third experiment, **Run-NoArgo**, SLA, SST and all "other Non Argo Insitu data" are assimilated. No Argo data is assimilated.

For the above 3 experiments, the strategy is to start from the PSY3 operational system that assimilates all the data and withdraw part of the Argo dataset in the next experiment. Table 2 summarizes the experiment strategy.

- The fourth experiment is a free run, hereafter name **Free-Run**, where no data at all have been assimilated. The Free-Run is here to assess the overall performance of the Mercator Océan PSY3 analyzing system.

	SST	SLA altimetry	Argo	Other Non Argo Insitu
Run-Op	X	X	X	X
Run-NoArgo	X	X		X
Run-Argo2	X	X	50% of the array	X
Free-Run				

Table 2 : List of data assimilated in the various OSEs

Results

Impact of Argo observations on physical fields and specific ocean process.

We found that comparing the monthly mean physical field is a good way to focus on short time scale events such as deep convection that need Argo data assimilation to be correctly described in the PSY3 system. Specific ocean processes such as deep convection or outflow are largely impacted by Argo data assimilation.

One of the easiest ways to study the impact of the Argo observations on the PSY3 system is to compare analyzed temperature and salinity fields from Run-Op and Run-NoArgo. Figure 2 shows the difference of the monthly mean salinity in the 1000-2000m layer for the month of March 2012. At that depth, the global ocean is sparsely impacted by the Argo data assimilation (figure 2a). It seems that only high dynamic regions are strongly corrected by the analysis system. Figure 2b is a zoom in the Labrador Sea, where the impact is the largest.

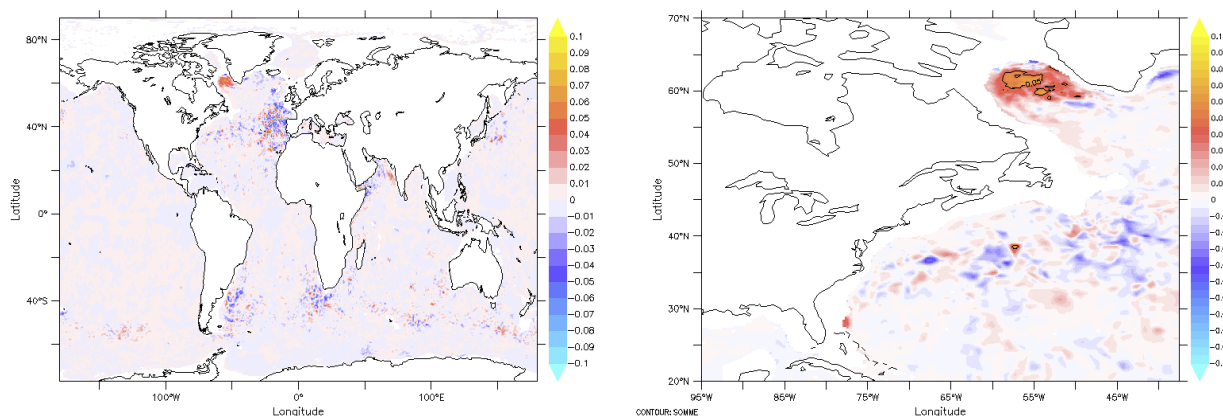


Figure 2 : Monthly (march 2012) difference between Run-Op and Run-NoArgo of the salinity analyzed fields (psu) averaged over layer 1000 and 2000m a) for the Global Ocean– b) zoom on the Labrador sea

Figure 3 presents two salinity time series of a numerical mooring (56.15°W – 60.58°N) in the Labrador Sea from the Run-Op and the Run NoArgo. It is striking that the descriptions of the convection episode greatly differ in the 2 experiments. With Argo data assimilation, the convection is shallower and very much shorter than without Argo data assimilation. The 38.85 psu contour reaches 700 meter depth with a short term episode in April 2012 at more than 1400m depth. Without Argo data assimilation, it reaches 1400m from February to June 2012. The re-stratification of the upper ocean is much slower when no Argo data are assimilated.

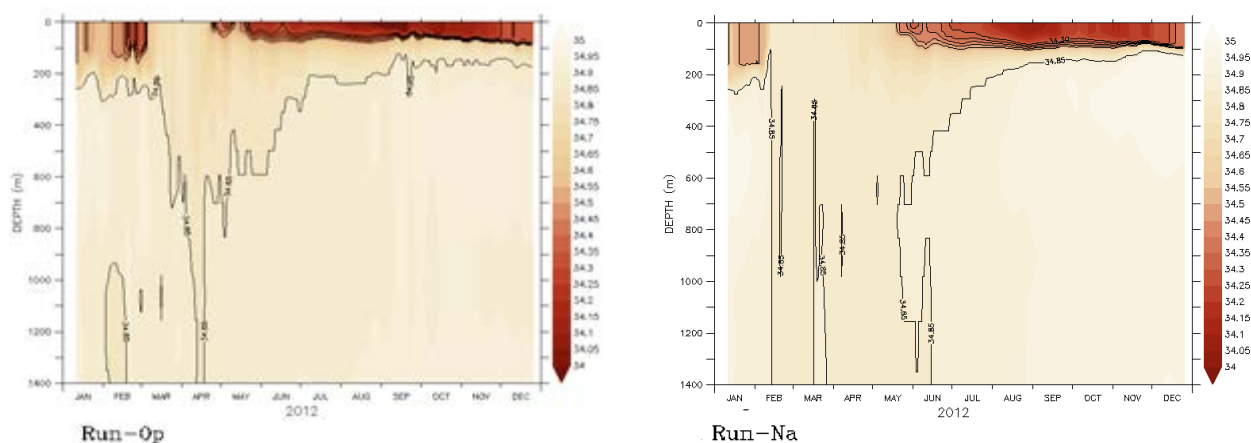


Figure 3 : Salinity (psu) time series in 2012 showing the deep convection episode in the Labrador sea a) Run-Op b) Run-NoArgo

Evaluate the location of the impact of Argo observation assimilation

Figure 4 displays a statistical view of the Argo data assimilation impact. The spatial distribution of the RMS (figure 4a) of the temperature differences between Run-Op and Run-NoArgo is calculated for the last 6 months of experiments in the 0-300m layer. Figure 4b is the spatial distribution of the Run-Op temperature standard deviation. It represents the variability of the system.

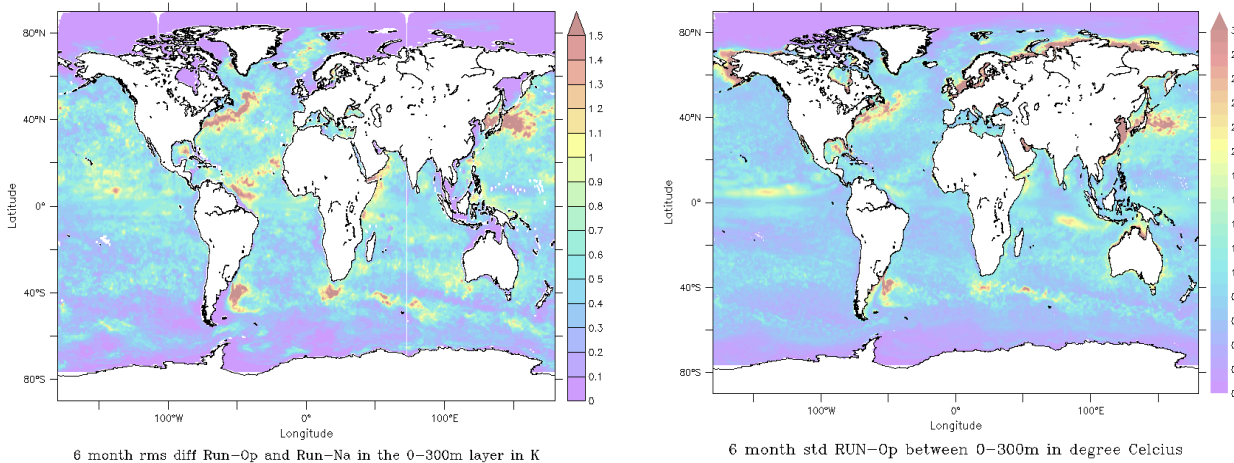
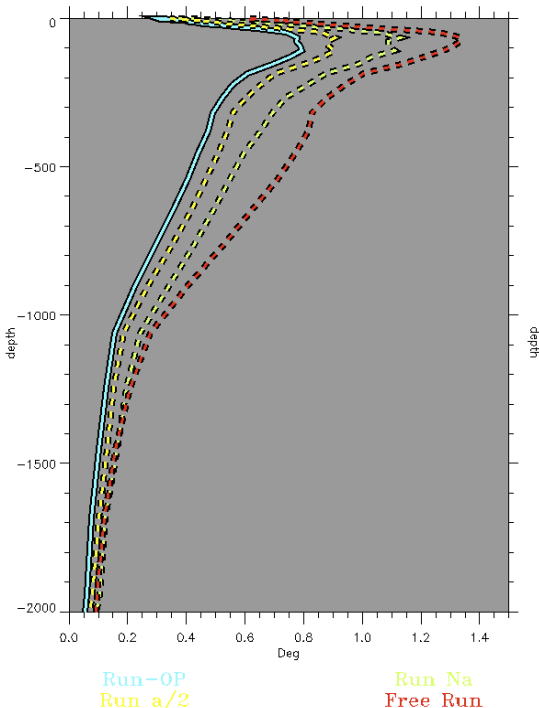


Figure 4 : a) RMS of temperature differences between Run-Op and Run-NoArgo in the 0-300m layer for the last 6 months of the 2012 experiment. b) STD of the Run-NoArgo in the 0-300m layer for the last 6 months of the 2012 experiment.

In the 0-300m layer, the global ocean is strongly impacted by the Argo data assimilation. The RMS reaches 0.5°C in many regions. Maximum values of the RMS (around 1.5°C) are strongly correlated to the regions where the variability (STD) is very high (Gulf Stream, Kuroshio, Brazilian current, and Agulhas current). Information brought by Argo data assimilation in these regions is strongly impacting the analyzed temperatures. The western tropical Atlantic is also highly impacted. This region combines the thermocline positioning process and the dynamic of the Amazon's outflow. Argo observations are necessary to constrain these processes.

It is necessary to have a statistical view of the analyzed field differences between 2 experiments. Comparing the spatial distribution of the RMS to the Standard deviation of the Run-Op put into perspectives the importance of the impact. Focusing on a particular layer is also necessary as the variability in the upper and lower ocean is very different from surface to depth.

Impact of Argo on the data assimilation results



In order to have a more synthetic view, we compare in Figure 5 in-situ observations to analyzed fields for the four experiments. The differences between in-situ observations and temperature fields after data assimilation is named misfit. Figure 5 is the mean profile of the RMS misfit calculated for the last 6 months of the 2012 experiment. In order to do so, we calculate the difference between model and all in-situ observations, assimilated or not. It is necessary to consider the same number of data for the calculation in order the experiments to be comparable to each other. Figure 5 shows the mean RMS temperature misfit of the global ocean, for the whole water column and for the 4 experiments. The improvement made by the assimilation is correlated to the number of data assimilated. The more data are assimilated, the better the performance of the system is. However, this is not totally true, in particular at depth, where the Free-Run RMS misfit is lower than the RMS misfit of the Run-NoArgo. It is interesting to see that without Argo data assimilation, the PSY3 system has a lower performance than the Free-Run. This is a good example of the importance of Argo in this PSY3 data assimilation system.

Figure 5 : mean global RMS profile of the temperature differences between analyzed fields (CyanBlue for Run-Op, green for Run-NoArgo, red for Free-Run and yellow for Run-Argo2) and observations from 0-2000m

Exploring the numerical deep Ocean

Observing System Experiments are also useful in order to anticipate the future of the Argo array. One of the next steps of the Argo development is to sample the deeper Ocean, down to 4000m depth. Evaluating the actual impact of Argo assimilation in the 2000m – 4000m layer (figure 6a) and comparing that impact to the variability of the ocean under 2000m (figure 6b) gives an interesting information on the future regions of interest for the deep sampling.

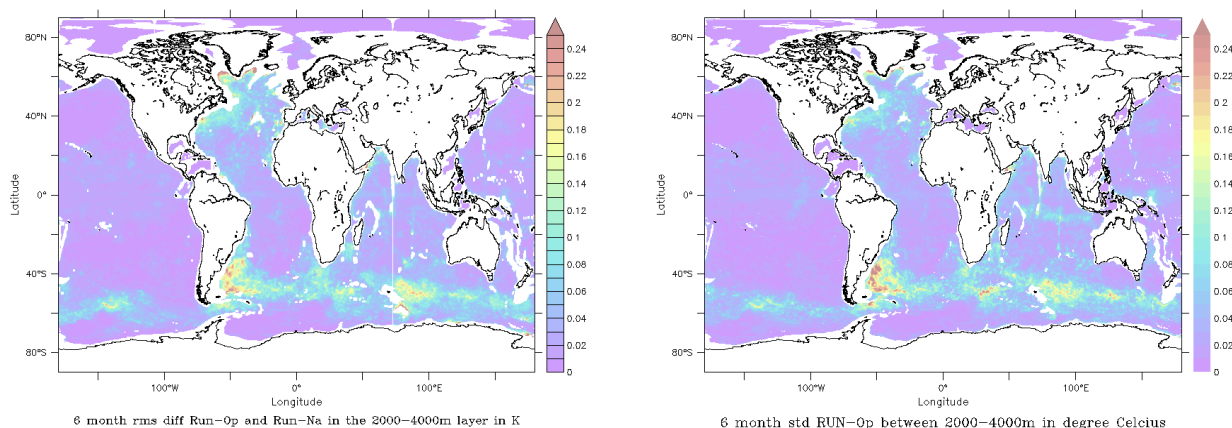


Figure 6 : a) RMS of temperature differences between Run-Op and Run-NoArgo in the 2000-4000m layer for the last 6 months of the 2012 experiment. b) STD of the Run-NoArgo in the 2000-4000m layer for the last 6 months of the 2012 experiment.

Regions with high variability seem already very impacted by Argo data assimilation, but, as no data are sampled at that depth, we do not know whether the correction is improving or degrading the solution. From the data assimilation point of view, sampling at that depth in these regions should be a priority. Also, figure 5 has shown that for the 1000m to 2000m layer, the Run-NoArgo is worse than the Free-Run. It hence appears essential to sample regularly the deep ocean and make sure that the system is not drifting from the reality.

Conclusion

The role of Argo observations on the PSY3 operational $\frac{1}{4}$ degree global forecasting system of Mercator Océan is absolutely essential. Figures shown have highlighted a series of results that assess the impact of Argo data assimilation on the PSY3 system. For example, considering the assimilation result, Argo data assimilation is reducing the RMS misfit from 20% to 40% depending on the depth.

In addition, several results presented here show the importance of Argo data assimilation for the control of the system. As an example, assimilating Argo at depth reduces the error introduced by the assimilation of satellite altimetry. Moreover, this study leads to a better understanding of how the data assimilation system works. For instance, the impact of Argo assimilation is highly correlated to the variability of the area, and is higher in regions of high variability. This remains to be further investigated in order to separate what originates from aliasing of variability in Argo data from the effect of larger model errors in these regions. Such investigations will contribute to design the future of the Argo array. Furthermore, we have seen that it becomes absolutely crucial to sample the deep ocean, even in low variability regions. From the operational oceanography point of view, modeling the deep ocean requires observations to constrain the analysis and to verify the reliability of the solution.

In this context, it sounds very difficult to reduce the Argo OSE into a few numbers of indexes. Argo observing system has a very large impact for operational oceanography and its importance is wider than the only "assimilation results". Nevertheless, highlighting the importance of Argo for ocean data assimilation as simply as possible is a necessity for the future of Ocean observing system and must push ourselves to imagine new ways, such as a dashboard of indicators, that will explain more completely the crucial role of Argo in our activity.

References

- C. Cabanes, A. Grouazel, K. Von chukmann, M. Hamon, V. Turpin, C. Coatanoan, S. Guinehut, C; Boone, N. Ferry, G. Reverdin, S. Pouliquen, P. Y. Le Traon: The CORA dataset: Validation and diagnostics of ocean temperature and salinity in situ measurement, *Ocean Sci.*, 2013
- J.M.Lellouche, O. Legalloudec, M.Drévillon, C. Régnier, E. Greiner, G. Garric, N. Ferry, C. Desportes, C-E. Testut, C. Bricaud, R. Bourdallé-Badie, B. Tranchant, M. Benkiran, Y. Drillet, A. Daudin and C. De Nicola, 2012: Evaluation of global monitoring and forecasting systems at Mercator Océan. *Ocean Science*, 9,1-25, 2013
- D. T. Pham, J. Verron, M. C. Roubaud: A singular evolutive extended Kalman filter for data assimilation in oceanography, *J. Mar. Syst.*, 16, 323-340, 1998
- R. W. Reynolds, T. M. Smith, C. Liu, D. B. Chelton, K. Casey and M. G. Schlax: Daily high-resolution blended analysis for sea surface temperature, *J. Climate*, 20, 5473-5496, 2007

Notebook

Editorial Board:

Laurence Crosnier and
Sylvie Pouliquen

DTP Operator:

BBS Studio

Articles:

Delayed mode analysis of argo floats: improvements of the method in the north atlantic and southern ocean

By C. Cabanes, V. Thierry, J. Lepesqueur, S. Speich, C. Lagadec

Zonal jets at 1000m in the tropics observed from argo floats' drifts

By S. Cravatte, F. Marin, W. S. Kessler

Upper ocean salinity stratification in the tropics as derived from n₂, the buoyancy frequency

By C. Maes, and T. J. O'Kane

Monitoring the ocean with tara - a coriolis perspective

By M. Picheral, H. Legoff, V. Taillandier, S. Searson, C. Marec, G. Obolensky and S. Morisset

Elephant seals help us to better observe the southern ocean

By F. Roquet, S. Blain, C. Guinet, G. Reverdin

Observing system experiment: a simple tool to assess the multiple roles played by argo observations on the operational forecasting system of mercator océan

By V. Turpin, E. Remy, P-Y Le Traon

Contact :

Please send us your comments to the following e-mail address: webmaster@mercator-ocean.fr